Long title: Insights from the genomes of four diploid *Camelina* spp.

Sara L. Martin,[1] Beatriz Lujan Toro,[1] Tracey James[1], Connie A. Sauder[1], and Martin Laforest[2]

1 Ottawa Research and Development Centre, Agriculture and Agri-Food Canada, Ottawa, Ontario, Canada

2 Saint-Jean-sur-Richelieu Research and Development Centre, Agriculture and Agri-Food Canada Saint-Jean-sur-Richelieu, Quebec, J3B 3E6 Canada

*Corresponding author

E-mail: sara.martin@agr.gc.ca; slwmartin@gmail.com

Orchid ID: 0000-0003-2055-6498

All assembled genomes will be available on publication from the National Center for Biotechnology Information as part of Bioproject PRJNA750147.

© Her Majesty the Queen in Right of Canada, as represented by the Minister of Agriculture and Agri-Food Canada

Short title: Insights from diploid *Camelina* genomes

Keywords: allopolyploidy, chromosome evolution, genome evolution, phylogenomics, Camelina, Brassicaceae

Ottawa Research and Development Centre

1016, 960 Carling Avenue, Ottawa

Ontario, Canada K1A 0CA

Agriculture and Agri-Food Canada

Phone: 613-715-5406

Sara.Martin@agr.gc.ca

Abstract

Plant evolution has been a complex process involving hybridization and polyploidization making understanding the origin and evolution of a plant's genome challenging even once a published genome is available. The oilseed crop, *Camelina sativa* (*Brassicaceae)*, has a fully sequenced allohexaploid genome with three unknown ancestors. To better understand which extant species best represent the ancestral genomes that contributed to *C. sativa*'s formation, we sequenced and assembled chromosome level draft genomes for four diploid members of *Camelina*: *C. neglecta C. hispida* var. *hispida*, *C. hispida* var. *grandiflora* and C. *laxa* using long and short read data scaffolded with proximity data. We then conducted phylogenetic analyses on regions of synteny and on genes described for *Arabidopsis thaliana,* from across each nuclear genome and the chloroplasts to examine evolutionary relationships within *Camelina* and *Camelineae*. We conclude that *C. neglecta* is closely related to *C. sativa*'s sub-genome 1 and that *C. hispida* var. *hispida* and *C. hispida* var. *grandiflora* are most closely related to *C. sativa*'s sub-genome 3. Further, the abundance and density of transposable elements, specifically *Helitrons*, suggest that the progenitor genome that contributed *C. sativa*'s sub-genome 3 maybe more similar to the genome of *C. hispida* var. *hispida* than that of *C. hispida* var. *grandiflora*. These diploid genomes show few structural differences when compared to *C. sativa*'s genome indicating little change to chromosome structure following allopolyploidization. This work also indicates that *C. neglecta* and *C. hispida* are important resources for understanding the genetics of *C. sativa* and potential resources for crop improvement.

Introduction

A key goal in evolutionary biology is understanding the evolution of genomes - how changes in structure and content affects the rate of evolution (Otto and Whitton 2002). Three

linked processes shape genome structure: hybridization (Stebbins 1968; Rieseberg 1997; Soltis and Soltis 2009; Abbott et al. 2013), polyploidization (de Wet 1971; Levin 1983; Soltis and Soltis 1999; Husband et al. 2013) and chromosomal rearrangements (Rieseberg 2001; Rieseberg and Willis 2007). Crop genomes such as maize, canola, soybean, sugarcane and wheat (Schmutz et al. 2010; Schnable et al. 2011; Chalhoub et al. 2014; The International Wheat Genome Sequencing Consortium 2014) have underscored the frequency of these processes. While less effort has focused on diploid wild crop relatives (Michael and VanBuren 2015), sequencing the extant representatives of crop progenitors can provide insight into the crop's origins and genomic evolution (Marcussen et al. 2014; Latta et al. 2019).

The oil seed crop and allohexaploid *Camelina sativa* (L.) Crantz (2n = 40) has been sequenced and well described (Kagale et al. 2014). It's three parental genomes are thought to have diverged from each other recently between 2.5 Mya (Žerdoner Čalasan et al. 2019) and 5.4 Mya (Kagale et al. 2014) with the dates of the hybridizations contributing to *Camelina sativa*'s formation estimated as 5-10,000 years ago (Kagale et al. 2014). The *Camelina* genus includes four taxa with known diploid chromosome counts: *Camelina neglecta* (2n = 12, 1C = 265 Mb) J. Brock, Mandáková, Lysak & Al-Shehbaz, *Camelina laxa* C. A. Mey. (2n = 12, 1C = 275 Mb), *Camelina hispida* Boiss. var. *hispida* (2n = 14, 1C = 355 Mb) and *Camelina hispida* var. *grandiflora* (Boiss.) Hedge (2n = 14, 1C = 315 Mb) (Al-Shehbaz 2012; Martin et al. 2017; Brock et al. 2019). These species could be modern representatives of genomes involved in *C. sativa*'s formation.

While determining the origin of a polyploid lineage is generally difficult (Kyriakidou et al. 2018; Rothfels 2021), our knowledge of the ancestral chromosome structure of the Camelineae provides an opportunity to investigate related diploid genomes. In the 2000's,

researchers defined 24 large conserved collinear regions or blocks (Ancestral Crucifer Karyotype or ACK) among crucifer genomes (Schranz et al. 2006; Murat et al. 2015; Lysak et al. 2016) and reconstructed an ancestral karyotype with 8 chromosomes similar to *Arabidopsis lyrata* (L.) O'Kane & Al-Shehbaz (Koch and Kiefer 2005). These blocks were later grouped into 16 ancestral karyotype regions (ABK) corresponding to ancestral chromosome arms (Murat et al. 2015). *Camelina sativa*'s sub-genomes each show a conserved ACK structure, with 21 in-block breaks that, most likely, occurred in its progenitors (Lysak et al. 2016). Here we extend our understanding of the evolution of *C. sativa* by assembling draft genomes for *C. neglecta*, *C. laxa*, *C. hispida* var. *hispida* and *C. hispida* var. *grandiflora.* Using this data and the ACK structure we phase *C. sativa*'s sub-genomes and examine relationships within the Camelineae using a phylogenetic analysis before delving further into *C. sativa's* potential paternal lineage using transposable element abundance.

Materials and Methods

Plant Material and Nucleic Acid Isolation

Camelina neglecta, C. hispida var. hispida, C. hispida var. grandiflora, and *C. laxa* seed were obtained from the North Central Regional Plant Introduction Station (NCRPIS) (PI650135, PI650139, PI650133 and PI633185, respectively). Seeds obtained from NCRPIS were stratified in petri dishes using filter paper that was moistened with 0.2% KNO_3, sealed with Parafilm (Pechiney Plastic Packaging Company, Illinois, USA), and placed at 4°C in the dark for 2 weeks. For seed germination, the plates were then placed at room temperature under growth lights with a 16 h/8 h day/night light cycle. Seedlings were then sown on soil (soil, peat, and sand; 1:2:1; Promix, Rivière-du-Loup, Québec, Canada) with a photoperiod of 16 h 20°C days/8 h 18°C nights. For the largely self-incompatible species, *C. hispida* and *C. laxa,* rosette leaves were

sampled using dry ice for DNA extractions and stored at -80. For the self-compatible, *C. neglecta*, after 6 weeks, the plants were placed for another 6 weeks at 4°C with an 8 h/16 h day/night photoperiod for vernalization. Plants were then transplanted to 5 in pots with the same soil and allowed to self-pollinate and set seed in a 16 h/8 h day/night photoperiod with 20°C days and 18°C nights. Following approximately 3 months, the mature seeds were collected and this process was repeated to obtain a fifth-generation inbred line before sampling and storage. Vouchers for each of the accessions used have been deposited in the DAO (Department of Agriculture Ottawa) herbarium (*C. neglecta* DAO 902176; *C. laxa*: DAO 902754; *C. hispida* var. *hispida*: DAO 902780; and *C. hispida* var. *grandiflora:* DAO 902768).

For Pacific Biosciences long read (PacBio; Pacific Biosciences, Menlo Park, CA, USA) and Illumina short reads (Illumina Inc., San Diego, California, U.S) sequencing, total DNA was extracted using a FastDNA Spin Kit (MP Biomedicals, Solon, OH), grinding was done in the FastPrep (MP Biomedicals) at 4.0 for 20 s, with the addition of one ceramic bead. Two DNA extractions were pooled for a total volume of 200 µl and precipitated with the addition of 20 µl 3 M NaOAc and 200 µl 100% ethanol. Following overnight incubation at -20°C, the DNA was centrifuged at 13,000 rpm at 4°C for 30 min. The ethanol was decanted and the DNA pellet was washed with cold 70% ethanol, dried at 37°C for approximately 20 min and re-suspended in 100 µl 5 mM Tris-HCl (pH 8.5). The DNA concentration was determined by Qubit was 110 ng/µl. DNA quality was determined by running 1.0 µl on a 0.8% E-gel (Invitrogen by ThermoFisher) beside a 0.2 µg of 20kb ladder (GeneRuler 1kbPlus, ThermoFisher).

DNA was also extracted to generate sequence data using Oxford Nanopore Technologies (ONT; Oxford Nanopore Technologies, Oxford Science Park, UK). High molecular weight DNA extraction procedures were carried out as described in Workman et al. (Workman et al. 2018).

The Short Read Eliminator kit (Circulomics Inc) was used as per the directions.

Sequencing

Sequencing was conducted in five different locations. McGill University's Genome Quebec Innovation Centre completed PacBio sequencing using P6-C4 chemistry for *C. laxa*, *C. hispida* var. *hispida* and *C. neglecta*. A total of 7 Single Molecule Real-Time (SMRT) cells were used for sequencing *C. neglecta* and 8 cells each were used for *C. laxa* and *C. hispida*. They also generated paired end Illumina data for *C. laxa*, *C. hispida* var. *hispida* and *C. hispida* var. *grandiflora* with runs of 2 x 150 bases. The sequencing facility at the Microbial Molecular Technologies Laboratory (MMTL) in Ottawa (Ottawa Research and Development Centre, Agriculture and Agri-Food Canada) was used for paired-end sequencing using Illumina MiSeq v3 chemistry with runs of 2 x 300 bases with 500bp inserts. The Centre for Applied Genomics, The Hospital for Sick Children, Toronto, Canada prepared and sequenced four additional libraries: one paired-end (PE) library with 550 bp inserts using a Nano kit (Illumina, San Diego, CA, USA) and three mate-pair (MP) libraries: 3kb, 5kb and 10kb inserts using the Nextera mate-pair kit (Illumina). All four libraries were sequenced on an Illumina HiSeq-2000 using v4 chemistry and flow cells with runs of 2 × 126 bases. ONT sequencing data was obtained using a MinION with one FLO-MIN106 flow cell run for 48h for each taxon in the Martin Laboratory. Base pair calling was completed with Guppy v. 3.2.2+9fe0a78 (Wick et al. 2019). Finally, library preparation for chromosome conformation capture (Hi-C) analyses used the Proximo Hi-C 2.0 Kit from Phase Genomics Inc. (Seattle, WA, USA) and sequenced using Ilumina HiSeq 4000.

Quality Control and* de novo *Genome Assembly

Raw PacBio and ONT reads were self-corrected and assembled using Canu v1.8 (Koren et al. 2016). The corrected error rate was set to 14.4% for both *C. hispida* var. *grandiflora*, where

we only had ONT data, and for *C. hispida* var. *hispida*. Draft assemblies were polished using Illumina data filtered and trimmed with trimmomatic v 0.33 (Bolger et al. 2014) and up to three iterations of Pilon v 1.23 (Walker et al. 2014) using bowtie2 v 2.3.4.3 (Langmead and Salzberg 2012) and Burrows-Wheeler Aligner (bwa) (Li 2013). For C. *hispida* and *C. laxa*, the program Purge Haplotigs (Roach et al. 2018) was used to reduce redundancy resulting from the heterozygosity.

The quality of the polished assemblies was evaluated with QUAST 5.0.2 (Gurevich et al., 2013). The completion of the assembly's gene space was evaluated using BUSCO v3.0.2 (Simão et al. 2015) using the embryophyta_odb10 database and the degree to which the assemblies had been successfully collapsed was further assessed with HapPy (Guiglielmoni et al. 2021). Final heterozygosity and error rates were calculated with samtools v 1.9 (Li et al. 2009) and SNP detection and phasing was completed with Princess v0.01 (Mahmoud et al. 2021).

The chloroplast genome for each species was extracted from the draft assemblies by aligning contigs with *C. sativa*'s chloroplast genome using nucmer v 4.0 from MUMmer v 4.0. Chloroplast contigs were ordered and oriented based on *C. sativa*'s chloroplast and merged into a consensus using a custom script written in R.

Genome Scaffolding

Phase genomics used their proprietary software, Proximo, to produce chromosome level scaffolds (Oddes et al. 2018) for *C. neglecta*, *C. hispida* var. *hispida* and *C. laxa*. The scaffolding tool, ntJoin 1.0.3-0 (Coombe et al. 2020), was used to scaffold the genome of *C. hispida* var. *grandiflora* using the Hi-C scaffolded assembly of *C. hispida* var. *hispida*. A final round of polishing by Pilon was completed following scaffolding.

All genomes are available from as part of Bioproject PRJNA750147.

Phylogenetic analysis of* C. sativa *sub-genomes and Camelineae diploids

We determined the phylogenetic relationships among genomes for 1) diploid members of the Camelineae: *Arabidopsis lyrata* (Ensembl Genomes version 1.0), *Capsella rubella* (NCBI v. ANNY00000000.1), *Neslia paniculata* (L.) Desvaux (S. Wright personal communication) 2) the three sub-genomes of *C. sativa* (NCBI version JFZQ0000000.1) and 3) the four diploid *Camelina* species sequenced here. We used three methods to extract regions of the genomes for analysis. First we identified random fragments within homologous regions of the genomes, second we used a reciprocal best hit method to identify shared genes from *Arabidopsis thaliana* (TAIR version 10), and third we used Orthofinder 2.3.11 (Emms and Kelly 2017; Emms and Kelly 2019).

For the first approach shared homologous regions within each ACK block as described in the *A. lyrata* genome (Schranz et al. 2006) were isolated (Table S1). Each ACK region was cut into 1000 bp fragments, aligned to *A. lyrata*'s genome using bowtie2 (Langmead and Salzberg 2012) and filtered. Pairwise collinearity between this set of filtered fragments and each taxon was determined using nucmer from MUMmer (v4.0) then a custom R script determined which fragments that overlapped between all genomes and were found in three copies within a consistent set of *C. sativa*'s chromsomes (Table S2). Each set was aligned using msa 1.18.0 (Bodenhofer et al. 2015) and run in MrBayes v3.2.1 using a stepping stone model run for 6,000,000 generations to determine the appropriate model (Ronquist et al. 2012). We then ran the preferred model for 5,000,000 generations checking convergence of each run with the r package rwty (Warren et al. 2017). We then calculated seven metrics to exclude biased sequences or sources of misleading phylogenetic signal using TreeCmp 2.0 (Bogdanowicz et al. 2012) and TreSpEx 1.1 (Struck 2014). Specifically, following Nikolov et al. (2019) we calculated the number of matching splits and the Robinson-Foulds tree distances using TreeCmp; the upper

quartile and standard deviation of the long-branch scores, average patristic differences, and R^2 of the saturation score and slope with TreSpEx. Fragments were excluded from further consideration if they failed the convergence checks or were outliers for one or more of the seven phylogenetic metrics at the 99th percentile. For each set of trees belonging to ABKs located on the same chromosome or chromosome arm, we estimated species trees with ASTRAL-III (5.1.1) (Zhang et al. 2018).

Our second method used the information phasing the sub-genome structure of *C. sativa* as determined by the fragments above, to identify reciprocal best hits (RBH) (Chen et al. 2017) for *A. thaliana* genes in each genome and sub-genome. Specifically, sequences for genes identified for *A. thaliana* in the TAIR 10 assembly (available from www.arabidopsis.org) were used to extract similar sequences for each genome. Following recommendations by Chen et al. (2017) BLAST 2.2.31 (Altschul et al. 1990) hits for *A. thaliana* genes were screened (e-value of less or equal to 0.0001, 70% or more of the query length, 70% or greater identity with query, a bit score ratio between the first and second BLAST hit of 1.2 or greater) extracted from each target genome and BLASTed back to *A. thaliana*'s genome and filtered again with the additional criteria of aligning to the gene's original location.

The phylogenetic analysis of these best hits was then completed as above using MrBayes and ASTRAL-III by ABK. In addition, we randomly selected one sequence from each ACK 25 times to be a set of unlinked data and analyzed these using StarBEAST2 2.6.3 (Ogilvie et al. 2017; Suchard et al. 2018; Bouckaert et al. 2019), PhyloNet 3.8.2 (Than et al. 2008; Wen et al. 2018; Cao et al. 2019) and to generate a consensus tree with ASTRAL-III. StarBeast2 was run for between 20 and 100 million generations as required to produce estimated sample sizes (ESS) values above 200 with the GTR site model using a configuration file created by BEAUti 2.6.3

(Bouckaert et al. 2019), convergence was examined with Tracer (1.7.1) (Rambaut et al. 2018), summarized with TreeAnnotator 2.6.3 (Bouckaert et al. 2019) and plotted with the densiTree function in the R package phangorn 2.5.5 (Schliep 2011). PhyloNet's MCMC_Seq command was run with chain lengths of between 20 and 80 million as required to produce ESS values above 200 and the maximum number of reticulations set to 4. Networks and trees produced by PhyloNet were visualized using plotTree function from the package phytools 0.7.20 (Revell 2012).

Finally, AUGUSTUS 3.3.2 (Stanke et al. 2006) was run on the final version of the assembled genomes, reference genomes, and *Camelina sativa*'s phased sub-genomes to predict genes *in silico* using *Arabidopsis*. Amino acid sequences were then provided to OrthoFinder (Emms and Kelly 2019), which estimated the species tree.

Entire chloroplast genomes for *Arabis alpina*, *Arabidopsis thaliana*, *A. lyrata*, *Capsella bursa-pastoris*, *C. grandiflora*, *C. rubella* and *Camelina sativa* were downloaded from the Chloroplast Genome Database (https://rocaplab.ocean.washington.edu/old_website/tools/cpbase) and aligned with the four *Camelina* chloroplasts using the msa function in R (see above). A consensus tree was then estimated with MrBayes as above. Annotation of the chloroplast genomes was completed with GeSeq 1.77 (Tillich et al. 2017) through CHLOROBOX website (https://chlorobox.mpimp-golm.mpg.de/index.html), using *Camelina sativa*, *A. lyrata*, and *Capsella rubella*'s chloroplasts as reference sequences. The chloroplast genomes with their annotations were then visualized with the website's OrganellarGenomeDRAW (OGDRAW) 1.3.1 (Greiner et al. 2019).

***Synteny between* Camelina *diploids and* C. sativa *and* A. lyrata**

To evaluate collinearity between the chromosome level draft genomes we used nucmer

with both *C. sativa* and *A. lyrata* as references for comparison and scripts written in R employing the package circlize 0.4.11 (Gu et al. 2014) to order and visualize the alignments.

Transposable Element Annotation

Transposable elements (TEs) were located using the Extensive *de novo* TE Annotator 1.8.3 (EDTA; Ou et al., 2010), EAHelitron 1.5.1 (Hu et al. 2019), LRT_FINDER/LTR_FINDER_parallel (Xu and Wang 2007; Ou and Jiang 2019) and LTRharvest (Ellinghaus et al. 2008). Data from these last two programs was processed with LRT_retreiver (Ou and Jiang 2018), which was used to calculate the LTR Assembly Index, (LAI) (Ou et al. 2018). We determined whether *Helitrons* detected in *C. sativa*'s sub-genome 3 were also detected in syntenic regions of *C. hispida var. hispida* and *C. hispida* var. *grandiflora* using a script written in R and output from EAHelitron and nucmer. Specifically, we examined all regions of synteny (determined by nucmer), determined if a *Helitron* was detected in the region (by EAHelitron using the presence of sequence CTAG and a GC rich hairpin), and examined sequence similarity for 1000 bp upstream of the 3' end. We considered any pairs with 80% identity to represents the same *Helitron* insertion event.

Additional software used

The version of R used was 3.6.3 (2020-02-29) -- "Holding the Windsock." Sequence handling, tree plotting and graphical display were facilitated by numerous R packages in addition to those mentioned above including: ape 5.0 (Paradis and Schliep 2019), apex 1.0.4 (Schliep et al. 2020), Biostrings 2.56.0 (Pagès et al. 2020), pals 1.7 (Wright 2021), pBrackets 1.0.1 (Schulz 2021), plotrix 3.7.8 (Lemon 2006), plyr 1.8.6 (Wickham 2011), ips 0.0.11 (Heibl 2008), IRanges 2.22.2 (Lawrence et al. 2013), outliers 0.14 (Komsta 2011), RIdeogram 0.2.2 (Hao et al. 2020), Rsamtools 2.4.0 (Morgan et al. 2020), seqinr 3.6.1 (Bastolla et al. 2007), stringr 1.4.0 (Wickham

2019), treeio 1.10.0 (Wang et al. 2020), and VennDiagram.1.7.1 (Chen 2021).

The program FigTree 1.4.4 (Rambaut 2018) was used to convert trees including their support values to a format easily readable in R.

Unless otherwise specified all tools were run using default settings.

Results

Genome Assemblies

Sequencing coverage of the genome differed for each species with *C. neglecta* receiving the majority of our sequencing efforts (286x raw coverage) (Table 1). Following assembly with Canu and polishing with Pilon, *C. neglecta* had the most contiguous assembly with 204 contigs and an NG50 of 11,493,634 (Table 2). Scaffolding using Hi-C data and Phase Genomics' Proximo resulted in chromosome level assemblies for *C. neglecta* (n = 6), *C. hispida* var. *hispida* (n = 7) and *C. laxa* (n =6) with approximately 70% or more of their expected lengths and NG50s of 29,279,412. 39,460,631, and 31,147,072 respectively. Following scaffolding by ntJoin, 70% of the expected genome length for *C. hispida* var. *grandiflora* was incorporated into a chromosome level assembly (n = 7). The completeness of gene space, as evaluated by estimating the proportion of core conserved eukaryotic genes recovered by the Benchmarking Universal Single Copy Orthologs (BUSCO) score, indicated that all assemblies had at least 90% of the expected genes (Table 2). The small percentage of duplicated BUSCO genes indicated that the assemblies have largely been collapsed. This was confirmed by haploidy scores from HapPy of over 0.9. The genomes all rank as gold quality based the high level of intact LTR elements detected in the genome (LIA > 20) (Table 2).

Phylogenetic relationships among **C. sativa** *and Camelineae diploids*

In total 1,444 fragments within the ACK blocks described for *A. lyrata* genome were found to be shared among the eight core Camelineae taxa with three copies distributed across *C. sativa*'s genome. Fragments from each ancestral chromosome showed the same pattern of localization in *C. sativa*'s genome in the majority of cases (Table 3). For example ACK blocks A, B, and C from ancestral chromosome 1 all showed the highest number of hits on *C. sativa*'s chromosomes 3, 14 and 17. Where differences occurred, there was consistency corresponding to ancestral chromosome arms and, therefore, ABK group. The pattern of hits across the genomes resulted in eleven groupings, corresponding to either ancestral chromosome arms or entire chromosomes, that were used in further phylogenetic analyses (Table 4).

The species trees produced by coalescent modeling by ASTRAL-III from gene trees produced from all fragments within the eleven groups indicated the phylogenetic relationship between *C. sativa*'s chromosomes and the other taxa (Table 4; Table 5; Fig. 1). Trees were largely congruent as indicated by the high normalized quartet scores (Table 4).

The consensus species trees estimated by StarBEAST2 using the reciprocal best hit (RBH) sequences also most consistently recovered this topology (Fig. 2 and 3) as did the final species tree predicted by OrthoFinder based 14,513 genes trees (Fig. 4). Further, all methods indicated *Arabidopsis* is the basal genus in this group, while *Neslia* is closest genus to *Camelina* among those studied.

The primary uncertainty in tree topology was the position of *C. laxa* - either basal to all the *Camelina* spp. or in a clade with *C. sativa*'s sub-genome 3 and *C. hispida.* Specifically, of the randomly chosen sets of sequences from across the genome, ASTRAL-III consensus trees produced trees with *C. laxa* basal to the *Camelina* group just over half the time - 14 of 25 for the fragments and 15 of 25 for the reciprocal best hit genes. The consensus trees produced by

StarBEAST2 showed greater disparity with 18 of 25 suggesting *C. laxa* is basal for the fragments but only 6 of 25 for the RBH. A thin majority, 14 of 25, of the RBH suggested *C. laxa* in a clade with *C. sativa*'s sub-genome 3. This topology, with *C. laxa* in the sub-genome 3 clade, was also produced by Orthogene (Fig. 4). Density tree plots of trees generated by StarBEAST2 indicated mixed signals for *C. laxa*'s position for sequence fragments (Fig. 2A) and for genes (Fig. 2B). These plots also indicated that some trees differed in the timing of divergence in genes among *C. laxa*, *C. sativa*'s sub-genome 3, and the varieties of *C. hispida* (Fig. 2C). Both ASTRAL-III and StartBeast2 account for incomplete lineage sorting; however, given the propensity of Brassicaceae taxa to hybridize, reticulate evolution between these taxa was investigated with PhyloNet. However, for many of the sets of 24 unlinked fragments or genes, PhyloNet indicated trees without reticulations were the most credible for the fragments (10 of 25) and the reciprocal best hit genes (17 of 25). With other sets one reticulation was included in the credible networks, but their placement was inconsistent (Fig. 3).

Results for Chloroplasts

The chloroplast (cp) assemblies produced for the four diploid *Camelina* species sequenced here, based on the scaffolding of contigs using *C. sativa*'s cp, resulted in contigs between 152,239 bp (*C. hispida var. grandiflora*) and 153,366 bp (*C. neglecta*) in comparison to the 153,044 bp for *C. sativa's* cp assembly. Annotation by GeSeq indicated expected features such as the large inverted repeat and that ARAGORN 1.2.38, invoked by GeSeq, found the same 39 genes in all four of the *Camelina* cp's assembled here and that of *C. sativa*. The cp assemblies varied in the degree of fragmentation of the genes within the assembly with *C. hispida var. grandiflora* showing the greatest number of fragmented features (89) and *C. neglecta* the fewest (20) (Fig. S1). The resulting tree from entire chloroplast sequences of all eleven taxa included in

the analysis, showed the chloroplast sequence from *C. sativa* was most closely related to that of *C. neglecta* and that these taxa were sister to a clade containing the varieties of *C. hispida* with *C. laxa* basal. As with the analysis of nuclear genes, the chloroplast indicates *Capsella* as more closely related to *Camelina* than *Arabidopsis* (Fig. 5).

Synteny between Camelina diploids and A. lyrata and C. sativa

The four diploid species sequenced here showed extensive synteny with both *A. lyrata* and *C. sativa* genomes with conservation of the ACK and ABK blocks (Fig. 6). The analysis indicates a high level of synteny between *A. lyrata* and *C. neglecta*, and to a greater degree, between *C. neglecta* and *C. sativa* sub-genome 1 (Fig. 6). Similarly, there is strong synteny between *A. lyrata* and *C. hispida* and, to a greater extent, between *C. hispida* and *C. sativa* sub-genome 3 (Fig. 6). In contrast the genome of *C. laxa* has more extensive rearrangements and breaks within ACK and ABK blocks (Fig. 7) including fragmentation of the E block, and separation of parts of the F, J, U, and W blocks on to separate chromosomes. Further, chromosome number reduction in this species involved portions of several of the ancestral chromosomes have being incorporated into several different chromosomes such as the upper arm of chromosome 6 - AK06 (FG) which has been split between chromosomes 3 and 5.

Transposable element annotation and comparison

Annotation of the transposable elements (TEs) by the Extensive *de novo* TE Annotator (EDTA) indicated that TEs made up 34-35% of the diploid *Camelina* genomes, with the exception of *C. hispida* var. *hispida* where TEs accounted for 50% of the genome (Fig. 8, Table S2). The largest groups of TEs identified belonged to the *Helitron* (DHH) and *Gypsy* superfamilies (RLC). EAHelitron identified fewer *Helitrons* than EDTA (Table 6). However, the

difference in the number of *Helitrons* in *C. neglecta* and *C. hispida* var. *hispida* was even more divergent with *Helitron* densities of 9.6 and 20.4 per 1,000,000 bp respectively. The percentage of *Camelina hispida* var. *grandiflora*'s genome (34%) and the *Helitron* density (11.8) was much lower than that of *C. hispida* var. *hispida* (Table S2). The three sub-genomes of *C. sativa* also showed differences in the number of TEs and specifically *Helitrons*, with sub-genome 1 and 2 showing similar percentages of TEs at 30.2% and 26.6% and similar *Helitron* densities at 6.1 and 5.8, but sub-genome 3 showing higher values at 40% and 14.7. In syntenic regions, *C.sativa* shared more *Helitrons* with *C. hispida* var. *hispida* (258) than with *C. hispida* var. *grandiflora* (178) (Table 7, Fig 9).

Discussion

Whole genome sequencing is allowing a deeper understanding of the processes that have shaped plant evolution including polyploidization, hybridization and chromosomal rearrangements. Allopolyploid crops have become excellent systems for understanding these genomic changes because they have often received substantial sequencing effort (e.g. *Triticum aestivum* L. (Appels et al. 2018), *Solanum lycopersicum* L. (Sato et al. 2012), *Zea mays* ssp. *mays* L. (Schnable et al. 2009; Jiao et al. 2017), and *Arachis hypogaea* L. (Bertioli et al. 2019)). Moreover, as work on these species has shown, a greater understanding of the genomic changes associated with allopolyploidization or autopolyploidization, the genomic consequences of domestication, and the potential breeding resources can be achieved when related, extant diploid species are also sequenced (e.g. Sato et al. 2012; Marcussen et al. 2014; Bertioli et al. 2016; Ramos-Madrigal et al. 2016).

The genome of the allohexaploid *Camelina sativa* (L.) Crantz (camelina; 2n = 40) has been sequenced (Kagale et al. 2014), but extant relatives of the three parental genomes have not.

Four diploid taxa are known within the genus: *Camelina neglecta*, *Camelina laxa*, *Camelina hispida* var. *hispida* and *Camelina hispida* var. *grandiflora*. Here we sequenced the genomes of these four diploids, assembled high quality chromosome level drafts, and examined their phylogenetic relationship with *C. sativa's* sub-genomes. Each genome showed synteny with *A. lyrata* with conservation of ACK and ABK blocks, with each region mapping once, confirming a diploid structure (Fig. 6, 7). This conservation of ACK and ABK blocks allowed for further dissection of the genomes and phylogenetic analysis.

Camelia sativa's Sub-genomes

Species trees produced by ASTRAL-III's multi-species coalescent model using trees produced from sequence data from each ABK or ACK indicated the phylogenetic relationships between these regions from *C. sativa*'s chromosomes and the other taxa included (Fig. 1). These phylogenies indicate that the phasing of *C. sativa*'s chromosomes to sub-genomes required reassessment compared to that originally suggested by Kagale et. al (2014). Given that rearrangement and fractionation have not been predominant mechanisms of genome change in *C. sativa* (Lysak et al. 2016), limited visual information is available for this division. Phasing polyploid genomes into their sub-genomes remains a challenging issue (Rothfels 2021) and the majority of tools to aid in this are currently only able to handle tetraploids (e.g. AlloppNET) (Jones 2013). Here, phasing was accomplished by using the distribution of ancestral syntenic blocks and placing them in phylogenetic context with related diploids. This allowed us to define sub-genome 1 as composed of the chromosomes with the closest phylogenetic relationship with *C. neglecta*, sub-genome 2 as those chromosomes sister to the clade with *C. neglecta* and sub-genome 1, and sub-genome 3 as chromosomes with the closest phylogenetic relationship to the

varieties of *C. hispida* (Table 4; Table 5; Fig. 1). This is a different nomenclature than our previous work which defined sub-genome 2 as most closely related to *C. neglecta* (Lujan Toro 2017), but it is concordant with the revised sub-genome definition recently published for *C. sativa* (Chaudhary et al. 2020).

In Chaudhary et al.'s analysis (2020), the authors characterized 193 accessions of *Camelina*, including *C. neglecta*, *C. laxa*, *C. hispida*, *C. rumelica* Velen., tetraploid and hexaploid *C. microcarpa* Andrz. ex DC., and *C. sativa*, using a genotyping by sequencing (GBS) approach that mapped SNPs in sequences for these accessions to *C. sativa*'s genome. They determined that sequences from *C. neglecta* aligned to six of *C. sativa*'s chromosomes and tetraploid *C. microcarpa* aligned with 13 of the chromosomes. However, they determined that alignment reads did not correspond to the sub-genome structure published in Kagale et. al (2014) and refined the composition of the sub-genomes accordingly with *C. neglecta* sequences aligning to sub-genome 1, the tetraploid *C. microcarpa* sequences aligning to sub-genomes 1 and 2, and *C. hispida* partially aligning to sub-genome 3 (Chaudhary et al. 2020). As a result very different approaches, an analysis based on SNPs and a phylogenetic analysis of whole genome sequences, has resulted in the same conclusions about refinements to the sub-genome structure of *C. sativa*.

In all three sub-genomes, the majority of the changes in the genome structure in comparison to *A. lyrata* are shared between the diploid genomes and the sub-genomes of *C. sativa* (see below, Fig. 6, 7). This conservation of structure in these closely related genomes is in line with Lysak et al.'s expectations that the majority of the changes in chromosome structure seen in *C. sativa* compared to the ancestral chromosomes were likely present in the ancestral diploid genomes (Lysak et al. 2016). While the formation of *C. sativa* was relatively recent (Kagale et al. 2014), it is clear that allopolyploidization did not result in extensive structural

reorganization of the genome, but rather can be characterized by conservation of ancestral chromosome structure and gene order.

Inter-genome recombination has been observed in some allopolyploids, including resynthesized *Brassica napus* (Pires et al. 2004), and if this has occurred in *C. sativa*'s genome it could result in conflicting signals in some loci, as could historical gene flow and introgression. Some genes appear to show a signal of hybridizations among *C. laxa*, *C. sativa*'s sub-genome 3 and the varieties of *C. hispida* (Fig 2., Fig 3.), and further evaluations of this possibility could be completed with broader, population level sampling of the taxa and evaluation of the evidence of introgression (Martin et al. 2015; Martin and Jiggins 2017; Crowl et al. 2020).

***Camelina neglecta* - an extant, maternal relative**

With the refinements to the phasing of the sub-genome structure of *C. sativa*, in addition to the close phylogenetic relationship, there is strong synteny between the draft *C. neglecta* and *C. sativa*'s sub-genome 1 (Fig. 6) with similar conservation of the ancestral chromosome structure. Specifically, only two large inversions are apparent when *C. neglecta*'s genome and *C. sativa*'s sub-genome 1 are compared: one at the start of *C. neglecta'*s chromosome 6 and end of *C. sativa's* chromosome 8 and one within *C. neglecta'*s chromosome 2 and *C. sativa's* chromosome 7, which is echoed in the homologous chromosome of *C. sativa*'s sub-genome 2. Interestingly, the inversion in *C. neglecta'*s chromosome 6 is more similar *A. lyrata*'s chromosome 6 suggesting this change may have occurred in *C. sativa*'s genome 1 following allopolyploidization. This similarity and the chloroplast data, which suggests the maternal lineage of *C. sativa* is most closely related to *C. neglecta*, indicates that *C. neglecta* is a close extant, maternal relative of *C. sativa*'s sub-genome 1.

C. neglecta is also the closest relative of sub-genome 2 (Fig. 6) with the largest difference in structure the lack of fusion in *C. sativa*'s chromosomes 10 and 18 compared to *C. neglecta'*s chromosome 5 and several additional areas of inversions within *C. neglecta'*s chromosome 3. This suggests that the taxon that contributed *C. sativa*'s sub-genome 2 is or was a close relative of *C. neglecta* that retained the ancestral chromosome structure of n = 7 reconstructed for the genus by Mandáková et al. (2019). This taxon is currently unknown, but given that *C. neglecta* was only recently described as a distinct species because of its morphological similarity to *C. microcarpa*, it is possible that the taxon has been collected, but is similarly cryptic and not yet identified as distinct from accessions of *C. microcarpa*.

***Camelina hispida* - an extant, paternal relative**

The varieties of *C. hispida* show a close phylogenetic relationship with *C. sativa's* sub-genome 3 (Fig 7). There is extensive synteny among these genomes indicating strong preservation of chromosome structure and gene order (e.g. Fig. 7). As in the comparisons between *C. neglecta* and *C. sativa*'s genomes 1 and 2, three chromosomes appear to have inversions, one of which is shared in comparisons with *A. lyrata* and potentially represents a change since *C. sativa's* formation. While the phylogenies indicate that both varieties of *C. hispida* share a common ancestor with *C. sativa*'s sub-genome 3, the frequency of TE elements differs strongly between the two varieties and is responsible for the 12% larger 2C DNA content of in *C. hispida* var. *hispida* (Martin et al. 2017).

The frequency of TEs and, in particular, shared *Helitrons* suggest *C. hispida* var. *hispida*'s genome may more closely resembles the genome that contributed *C. sativa's* sub-genome 3. The frequency of TEs varies across *C. sativa*'s sub-genome's with sub-genome 3

having the highest number of these elements, at 40% of the sub-genome, compared to 30% in the other two (Fig. 8., Table 6, SI Table 2). Among the diploids sequenced here this percentage is closest to the percentage observed for *C. hispida* var. *hispida* (50%). The largest portion of these TEs by count, *Helitrons*, make up 15% of *C. sativa*'s sub-genome 3 and 16% of *C. hispida* var. *hispida's* genome. *Helitrons* were first discovered in the genomes of *Arabidopsis thaliana*, *Oryza sativa* L. and *Caenorhabditis elegans* Maupas (Kapitonov and Jurka 2001) and are the most abundant TEs in *A. thaliana*'s genome. They make up the second largest TE portion of the genome after the less numerous, but longer retro-elements such as *Copia* and *Gypsy* (Quesneville 2020). Hu et al. (2019) have suggested that, because *Helitron* density is highly evolutionarily labile they could be used for species identification. In this case, we investigated whether they may provide clues to which genome was more similar to that which contributed to the formation of *C. sativa*. We used the software developed by Hu et al. (2019), EAHelitron, to determine whether *Helitrons* detected in *C. sativa*'s sub-genome 3 were more often shared with *C. hispida* var. *hispida* or *C. hispida* var. *grandiflora*. This indicated that 7.5% of the *Helitrons* in *C. sativa*'s sub-genome 3 are shared with *C. hispida* var. *hispida*, while 5.2% are shared with *C. hispida* var. *grandiflora's* (Table 7, Fig. 9). This suggests that the genome that contributed *C. sativa*'s sub-genome 3 may have been was more similar to the genome of *C. hispida* var. *hispida* with its higher TE content. However, it is also possible that with the large expansion of TEs in *C. hispida* var. *hispida's* genome, shared *Helitrons* were more likely to be retained.

Here we see reduced TEs abundance and *Helitron* density in sub-genome 3 from levels observed in *C. hispida* var. *hispida* and in sub-genome 1 compared to *C. neglecta*. However, one expectation is that genomic shock and relaxed selection pressure following allopolyploidization allows an increase in TE abundance (Parisod and Senerchia 2012; Vicient and Casacuberta

2017). For example, proliferation of TEs has been observed in allotetraploid *Coffea arabica* L.. Specifically, *copia* elements have increased the size of sub-genome C compared to that observed in the diploid representative, *C. canephora* L., a representative of the progenitor genome (Yu et al. 2011). Similarly, the transposon *Sunfish*, was observed to be released from repression in the early generations of synthetic autopolyploids of *Arabidopsis thaliana* and *A. arenosa* (L.) Lawalrée as well as their allopolyploid derivative *A. suecica* (Fries.) Norrlin. However, the same was not true for other TE families in *A. suecica* (Madlung et al. 2005) and more recent work by Burns et al. (2021) concluded there was no upregulation in transposon activity in *A. suecica* compared to its ancestral species. Ågren et al. (2016) also determined that the allotetraploid *Capsella bursa-pastoris* did not show genome wide TE proliferation compared to its progenitors, though did note a higher abundance in retrotransposons in gene rich regions, and Sarilar et al. (2013) determined that early generations of synthetic allotetraploid *Brassica napus,* did not show increased activity in three groups of TEs. Interestingly, similar to our observation, Hu et al. (2019) observed that *Helitron* density was also lower in the sub-genomes of the allotetraploid *Brassica napus* L. compared to the extant representatives of the parental genomes *B. rapa* L. and *B. oleraceae* L.. Here, the repeatome of *C. sativa* is less complete than that of the diploid genomes assembled with long reads and this may mean that the *Helitrons* in *C. sativa*'s genome are underrepresented. Alternatively, the diploid lineages may have seen proliferation of TEs since *C. sativa's* formation. As in the systems explored above, resynthesis of *C. sativa,* could determine whether the apparent changes are repeatable. Further, the variation in TE abundance between *C. hispida* varieties and the presence of extant G1G3, *C. rumelica,* and G1G2, "*C. microcarpa* 4x", tetraploids (Mandáková et al. 2019; Chaudhary et al. 2020) in addition to the G1G2G3 hexaploid *C. sativa* provides an intriguing opportunity to use resynthesis to study TE

dynamics after allopolyploidization and investigate how if TE abundance contributes to sub-genome dominance (Bird et al. 2018; Alger and Edger 2020).

The results presented by Žerdoner Čalasan et al. (Žerdoner Čalasan et al. 2019) suggest that *C. anomala*, a taxon with unknown chromosome number, is sister to *C. hispida* raising the possibility that this species could also be a close relative of *C. sativa*'s sub-genome 3. However, the species has not been collected since the 1800s and remains largely a mystery.

Camelina laxa

Camelina laxa is morphologically distinct from the other taxa studied here with its flexuous or zig-zagging stems and also has the most diverged genome from the ancestral karyotype. It is clear from the phylogenetic evidence here and cytological evidence presented by Mandáková et al. (2019) that *C. laxa* and *C. neglecta* represent separate transitions from n = 7 to n = 6. In *C. laxa*, extensive chromosomal rearrangements occurred, resulting from chromosome shattering, while in *C. neglecta* chromosome reduction resulted from the fusion of two chromosomes (Mandáková et al. 2019). However, the position of *C. laxa* in the phylogenetic tree was the least stable element across all analyses with two main alternatives, either as basal to all other *Camelina* species sampled or as basal to the clade containing the varieties of *C. hispida* and *C. sativa*'s sub-genome 3. While Mandáková et al.'s (2019) analysis of 48 single copy genes using ASTRAL placed *C. laxa* in a clade with *C. hispida*, the consensus from previous work is that *C. laxa* should be considered basal to the other species of *Camelina*. For example, Brock et. al. (2018)'s maximum likelihood consensus phylogeny constructed from ddRADseq for 48 specimens from gene bank material and field collections of *C. sativa*, *C. microcarpa* hexaploids, *C. rumelica*, *C. laxa* and *C. hispida* placed *C. laxa* was basal to the other species. Similarly, a

neighbor joining tree produced using GBS data indicated *C. laxa* was basal except the G1G3 tetraploid *C. rumelica* (Chaudhary et al. 2020). Finally, in a more comprehensive analysis of the Camelineae, which included *C. alyssum* (Mill.) Thell. and *C. anomala* Boiss. & Hausskn. ex Boiss. as well as representatives from many other genera included in the tribe *Nelisa*, *Capsella*, *Arabidopsis*, *Catolobus*, *Pseudoarabidopsis*, and *Chrysochamela*, Žerdoner Čalasan et al. (2019) also placed *C. laxa* as basal to *Camelina*. As a result, the preponderance of evidence currently suggests that this, more diverged lineage, is basal to the *Camelina*.

Conclusion

As domestication has decreased genetic variability in *C. sativa* accessions (Manca et al. 2013) other members of the genus might be of value for the improvement of *C. sativa*. Here our results indicate that *C. neglecta* and *C. hispida* var. *hispida* could be useful species to investigate variation in traits such as seed size, disease resistance and oil profiles. However, the collections available for these species are limited and international efforts to collect and preserve a broader selection of germplasm for the genus should be considered as we look to these species as sources of desirable traits for the improvement of the crop species (Ford-Lloyd et al. 2011).

Data Availability

All assembled genomes are available from the National Center for Biotechnology Information as part of Bioproject PRJNA750147.

Acknowledgements

We would like to thank the ORDC growth facility team for support rearing the plant material, the ORDC Molecular Technology Laboratory for support with sequencing, and the U.S.

National Plant Germplasm System and GRIN-Global for conserving and providing the germplasm needed for this research. We thank Dr. S. Wright for sharing the draft genome sequence of *Neslia paniculata* and Julia Mata for help processing convergence data. Funding was provided by Agriculture and Agri-Food Canada as part of the project "Gene flow, diversity and relationships within the Brassicaceae: Focus on *Camelina*" (J-001029).

Table 1. Genome sizes (1C) as estimated from flow cytometry and the fold coverage (x) for the four genomes sequenced here provided by long read data (PacBio and ONT) and short read data including Illumina paired-end reads (PE) and Illumina mate pairs (MP) with upper limits of estimates of heterozygosity (H) and error rates (ER) calculated by GenomeScope from the Illumina data.

SPECIES	GENOME SIZE (MB)	PACBIO	ONT	ILLUMINA		RAW COVERAGE	GENOMESCOPE	
				PE	MP		H	ER
Camelina neglecta	265	38	60	92	96	286	0.17%	0.08%
Camelina hispida var. *hispida*	355	38	53	52	-	143	1.09%	0.15%
Camelina hispida var. *grandiflora*	315	-	32	64	-	96	2.14%	0.15%
Camelina laxa	275	57	74	47	-	177	1.36%	0.24%

Table 2. Statistics on genome assemblies for *C. neglecta*, *C. hispida* var. *hispida*, *C. hispida* var. *grandiflora,* and *C. laxa* generated by QUAST and BUSCO based on the embryophyta_odb10 database before and after scaffolding. The initial assembly values for *C. hispida* and *C. laxa* are for assemblies following assembly by Canu and reduction in the number of alternative contigs resulting from the heterozygosity of these genomes by Purge Haplotigs. All assemblies were polished with Pilon. Addition metrics are 1) the haploidy score (HapPy) with 1 indicating perfect collapse, 2) the LTR Assembly Index (LAI) (LTR_retriever) with scores > 20 indicating gold quality, 3) final error rate (samtools), 4) number of SNPs (PRINCESS) and 5) final heterozygosity (PRINCESS).

	Camelina neglecta		*Camelina hispida* var. *hispida*		*Camelina hispida* var. *grandiflora*		*Camelina laxa*	
ASSEMBLY STRATEGY	CANU	HI-C	CANU & PURGE HAPLOTIGS	HI-C	CANU & PURGE HAPLOTIGS	NTJOIN	CANU & PURGE HAPLOTIGS	HI-C
contigs (>= 0 bp)	204	6	747	7	1,072	7	900	6
contigs (>= 10000 bp)	157	6	703	7	896	7	785	6
contigs (>= 50000 bp)	139	6	552	7	748	7	530	6
Total length (>= 0 bp)	210,252,877	194,776,448	305,512,316	283,171,403	247,512,955	247,668,533	223,800,267	199,991,310
Total length (>= 10000 bp)	210,014,359	194,776,448	305,328,622	283,171,403	247,070,138	247,668,533	223,546,568	199,991,310
Total length (>= 50000 bp)	209,462,969	194,776,448	301,174,771	283,171,403	242,642,354	247,668,533	217,296,729	199,991,310
Largest contig	19,486,679	48,079,882	6,147,326	45,593,769	3,518,166	41,100,942	4,931,297	39,604,730
Total length	210,252,877	194,726,046	305512316	283,171,403	247,512,955	247,668,533	223,800,267	199,991,310
Estimated genome size	265,000,000	265,000,000	360,000,000	360,000,000	320,000,000	320,000,000	275,000,000	275,000,000
Percent of Expected	79%	74%	85%	79%	77%	77%	81%	73%
N50	13,701,387	30,499,177	1053466	41,586,011	477,640	37,976,760	651,797	31,824,321
NG50	11,493,634	29,279,412	843316	39,460,631	346,627	30,680,265	477,199	31,147,072
N's per 100 kbp	-	1	-	16	-	32,233	-	20
BUSCO	2,121	2,121	2,121	2,121	2,121	2,121	2,121	2,121
Complete (%)	2,082 (98)	2,084 (98)	2055 (97)	2,025 (96)	2,063 (97)	1,901 (90)	2,079 (98)	2032 (96)
Complete Single Copy (%)	2,051 (97)	2,055 (97)	1938 (91)	1,971 (93)	1,863 (88)	1,853 (88)	1,939 (91)	1,978 (93)
Complete Duplicated (%)	31 (1)	29 (1)	117 (6)	54 (3)	200 (9)	48 (2)	140 (7)	54 (3)
Fragmented (%)	14 (<1)	14 (<1)	28 (1)	43 (2)	18 (<1)	65 (3)	14 (<1)	18 (<1)
Missing (%)	25 (1)	23 (1)	38 (2)	53 (3)	40 (2)	155 (7)	28 (1)	71 (3)
Haploidy Score		0.99		0.97		0.96		0.94
LAI		21.1		25.7		27.6		22.0
Error Rate		0.004		0.007		0.02		0.007
SNPs		420,396		1,564,682		1,813,558		1,488,895
Heterozygosity		0.002		0.006		0.007		0.008

Table 3. Distribution of the top three chromosomes with successful alignments of fragments from each of *Arabidopsis lyrata*'s ACKs across the genome of *Camelina sativa* as determined by bowtie2 ordered by number of hits.

ACK	ABK	*Camelina sativa* TOP CHROMOSOME	*Camelina sativa* 2nd CHROMOSOME	*Camelina sativa* 3rd CHROMOSOME
A	AK2	3	14	17
B	AK2	14	3	17
C	AK1	3	14	17
D	AK3	7	16	9
E	AK4	7	16	9
F	AK6	1	15	19
G	AK6	1	15	19
H	AK5	15	1	19
I	AK7	7	16	9
J	AK8	5	6	4
K	AK9	4	6	9
L	AK9	4	6	9
M	AK10	9	6	4
N	AK10	4	6	9
O	AK11	2	13	8
P	AK11	13	2	8
Q	AK12	8	13	20
R	AK12	8	13	20
S	AK13	10	11	12
T	AK14	10	11	12
U	AK14	11	12	10
V	AK15	11	20	18
W	AK16	18	11	2
X	AK16	11	2	18

Table 4. Summary of ACK and ABK groups across *Camelina sativa*'s chromosomes based on bowtie hits showing preservation of ancestral genome structure across ABK regions, but movement of some regions across chromosomes. Chromosomes were assigned to sub-genomes based on summary trees constructed by MrBayes from the ACK fragments grouped by ABK using ASTRAL III. The normalized quartet score, indicating the similarity of trees from individual fragments (out of one), produced by ASTRAL-III is presented. Sub-genome 1 was defined as the genome with closest relationship to *C. neglecta* while sub-genome 3 was defined as that with the closest relationship to the *C. hispida* varieties.

ACK	ABK	SUB-GENOME 1	SUB-GENOME 2	SUB-GENOME 3	FRAGMENTS IN GROUP	NORMALIZED QUARTET SCORE
ABC	AK1/2	14	3	17	262	0.78
DE	AK3/4	7	16	9	98	0.80
FGH	AK5/6	19	1	15	269	0.79
I	AK7	7	16	9	28	0.82
J	AK8	4	6	5	104	0.77
KLMN	AK9/10	4	6	9	115	0.79
OP	AK11	8	13	2	37	0.80
QR	AK12	8	13	20	180	0.79
STU	AK13/14	11	10	12	202	0.78
V	AK15	11	18	20	19	0.80
WX	AK16	11	18	2	130	0.78

Table 5. Sub-genome structure of *C. sativa* based on phylogenetic relationships of AKB regions and diploid genomes determined here in comparison to the original structure proposed by Kagale et al. 2014.

	This Paper	**Kagale et al 2014.**
Sub-genome 1	Cs 14 Cs 07 Cs 19 Cs 04 Cs 08 Cs 11	Cs 17 Cs 16 Cs 15 Cs 04 Cs 13 Cs 11
Sub-genome 2	Cs 03 Cs 16 Cs 01 Cs 06 Cs 13 Cs 10 Cs 18	Cs 14 Cs 07 Cs 19 Cs 06 Cs 08 Cs 10 Cs 18
Sub-genome 3	Cs 17 Cs 15 Cs 09 Cs 05 Cs 02 Cs 20 Cs 12	Cs 03 Cs 05 Cs 01 Cs 09 Cs 20 Cs 02 Cs 12

Table 6. Results of *Helitron* (DHH) annotation by EAHelitron. *Helitron* density is calculated as the number of *Helitrons* detected in the genome for each 1,000,000 bp.

SPECIES	HELITRONS	HELITRON DENSITY
Camelina neglecta	1877	9.6
Camelina hispida var. *hispida*	5776	20.4
Camelina hispida var. *grandiflora*	2933	11.8
Camelina laxa	937	4.6
Camelina sativa sub-genome 1	1220	6.1
Camelina sativa sub-genome 2	1024	5.8
Camelina sativa sub-genome 3	3395	14.7
Arabidopsis lyrata	3242	16.7
Arabidopsis thaliana	665	5.6
Capsella rubella	1826	14.1
Capsella grandiflora	226	2.1
Capsella bursa-pastoris	2576	9.6
Neslia paniculata	1003	8.9

Table 7. The number of shared *Helitrons* detected by EAHelitron in *C. sativa*'s sub-genome 3 within regions of synteny among *C. sativa*'s sub-genome 3, *C. hispida* var. *grandiflora,* and *C. hispida* var. *hispida* chromosome.

C. sativa CHROMOSOME	*C. sativa* *HELITRON* COUNT	*HELITRONS* SHARED WITH		COMMON *HELITRONS*
		C. hispida var. *grandiflora*	*C. hispida* var. *hispida*	
Cs 17	516	24	31	9
Cs 09	518	29	41	17
Cs 15	456	27	38	7
Cs 05	513	27	59	14
Cs 12	505	21	35	12
Cs 02	496	27	29	9
Cs 20	391	23	25	7
Total	3395	178	258	75

Fig 1. Species Trees. These species trees were produced by ASTRAL-III using a multi-species coalescent model and trees produced by MrBayes for each fragment identified by bowtie 2's alignment of sequence fragments from *A. lyrata.* These are grouped within eleven ABK groups that correspond to either whole ancestral chromosomes or chromosome arms, that have been largely conserved. The ACK(s) included in each tree are indicated in the box to the left of each tree and the ancestral chromosome structure with division into ACK and ABK is shown in the lower right.

Fig. 2. Density tree plots. Density tree plots of 1,000 randomly chosen tree estimated by StarBEAST2 for a set of A) fragment sequences, and B) genes, C) two sets of reciprocal gene sequences.

Fig. 3. **Consensus networks.** The consensus networks generated with PhyloNet using one set of reciprocal gene sequences (A) and the three most credible networks contributing to this consensus (B-D) with the percentage of credible networks represented.

Fig 4. Trees from OrthoFinder. Phylogenetic trees generated by OrthoFinder based on *in silico* predictions of amino acids produced by AUGUSTUS A) a consensus of 14,513 gene trees with an inferred root and B) a concatenated multiple sequence alignment of 7,401 shared, single-copy genes. Node labels indicate support values for each bipartition with the higher levels of support for the concatenated data expected for the type of analysis.

Fig. 5. **Chloroplast Based Phylogeny**. Phylogeny constructed from whole chloroplast alignment using MrBayes. Node labels indicate posterior probabilities.

Fig. 6. Synteny Plots with *C. neglecta and C. sativa's sub-genomes 1 and 2*. Plots indicating regions of synteny as indicated by nucmer between *C. neglecta*, with *A. lyrata* (A), *C. sativa*'s sub-genomes (B, C, E) and between *A. lyrata and C. sativa's sub-genomes* (D, F). Plot B is coloured by alignment with *A. lyrata's* chromosomes, analogs for the ancestral chromosomes.

Fig. 7. Synteny Plots with *C. hispida* var. *hispida*, *C. laxa* and *C. sativa* sub-genome 3. Plots indicating regions of synteny as indicated by nucmer among the diploid *Camelina* species *C. hispida* var. *hispida* and *C. laxa* with *C. sativa*'s sub-genomes (A, D, G, H) and with *A. lyrata* (B, E , I). Synteny between *C. sativa* sub-genomes and *A. lyrata* are shown for comparison (C, F). Plot B and F are coloured by alignment with *A. lyrata's* chromosomes, analogs for the ancestral chromosomes.

Fig. 8. **Transposable Element Types and Abundance.** Types of transposable elements (TE) in A) *Camelina neglecta*, B) *C. laxa*, C) *C. hispida* var. *grandiflora*, D) *C. hispida* var. *hispida*, E) *Arabidopsis lyrata*, F) *C. sativa* sub-genome 1, G) *C. sativa* sub-genome 2, and H) *C. sativa* sub-genome 3, as annotated by Extensive De novo Transposable Element (EDTA). Pie graphs are scaled by the percentage of the genome attributed to TEs which at highest is 49.6% for *C. hispida* var. *hispida* (D). Classification of transposable element type follows the unified classification system for eukaryotic transposable elements that uses a three letter code indicating class, order and superfamily (34). Here these are divided into three groups: DNA transposons (DNA), which includes *Helitrons* (DHH); long terminal repeats (LTR), which includes retrotransposons RLC (*Copia*) and RLG (*Gypsy*); and miniature inverted transposable elements (MITES).

Fig. 9. *Helitron* Ideogram and Abundance. A) Density of *Helitrons* identified by EAHelitron across the sub-genome 3 of *C. sativa* with the locations of *Helitrons* shared by *C. hispida* var. *hispida, C. hispida* var. *grandiflora* or both indicated and B) Venn diagram of the number of *Helitrons* shared among *C. hispida* var. *hispida, C. hispida* var. *grandiflora* , and *C. sativa*'s sub-genome 3.

References

Abbott R, Albach D, Ansell S, Arntzen JW, Baird SJE, Bierne N, Boughman J, Brelsford A, Buerkle CA, Buggs R, et al. 2013. Hybridization and speciation. J Evol Biol. 26(2):229–246. doi:10.1111/j.1420-9101.2012.02599.x.

Ågren JA, Huang HR, Wright SI. 2016. Transposable element evolution in the allotetraploid capsella bursa-pastoris. Am J Bot. 103(7):1197–1202. doi:10.3732/ajb.1600103.

Al-Shehbaz IA. 2012. A generic and tribal synopsis of the Brassicaceae (Cruciferae). Taxon. 61(5):931–954.

Alger EI, Edger PP. 2020. One subgenome to rule them all: underlying mechanisms of subgenome dominance. Curr Opin Plant Biol. 54:108–113. doi:10.1016/j.pbi.2020.03.004. https://doi.org/10.1016/j.pbi.2020.03.004.

Altschul SF, Gish W, Miller W, Myers EW, Lipman DJ. 1990. Basic Local Alignment Search Tool. J Mol Biol. 215:403–410.

Appels R, Eversole K, Feuillet C, Keller B, Rogers J, Stein N, Pozniak CJ, Choulet F, Distelfeld A, Poland J, et al. 2018. Shifting the limits in wheat research and breeding using a fully annotated reference genome. Science (80-). 361(6403). doi:10.1126/science.aar7191.

Bastolla U, Porto M, Roman HE, Vendruscolo M. 2007. Seqin{R} 1.0-2: a contributed package to the {R} project for statistical computing devoted to biological sequences retrieval and analysis. In: Structural approaches to sequence evolution: Molecules, networks, populations. New York: Springer Verlag. p. 207–232.

Bertioli DJ, Cannon SB, Froenicke L, Huang G, Farmer AD, Cannon EKS, Liu X, Gao D, Clevenger J, Dash S, et al. 2016. The genome sequences of *Arachis duranensis* and *Arachis ipaensis*, the diploid ancestors of cultivated peanut. Nat Genet. 48(4):438–446. doi:10.1038/ng.3517.

Bertioli DJ, Jenkins J, Clevenger J, Dudchenko O, Gao D, Seijo G, Leal-Bertioli SCM, Ren L, Farmer AD, Pandey MK, et al. 2019. The genome sequence of segmental allotetraploid peanut *Arachis hypogaea*. Nat Genet. 51(5):877–884. doi:10.1038/s41588-019-0405-z. http://dx.doi.org/10.1038/s41588-019-0405-z.

Bird KA, VanBuren R, Puzey JR, Edger PP. 2018. The causes and consequences of subgenome dominance in hybrids and recent polyploids. New Phytol. 220(1):87–93. doi:10.1111/nph.15256.

Bodenhofer U, Bonatesta E, Horejs-Kainrath C, Hochreiter S. 2015. msa: an R package for multiple sequence alignment. Bioinformatics. 31(24):3997–3999. doi:10.1093/bioinformatics/btv176.

Bogdanowicz D, Giaro K, Wróbel B. 2012. TreeCmp: Comparison of trees in polynomial time. Evol Bioinforma. 2012(8):475–487. doi:10.4137/EBO.S9657.

Bolger AM, Lohse M, Usadel B. 2014. Trimmomatic: A flexible trimmer for Illumina sequence data. Bioinformatics. 30(15):2114–2120. doi:10.1093/bioinformatics/btu170.

Bouckaert R, Vaughan TG, Barido-Sottani J, Duchêne S, Fourment M, Gavryushkina A, Heled J, Jones G, Kühnert D, De Maio N, et al. 2019. BEAST 2.5: An advanced software platform for Bayesian evolutionary analysis. PLoS Comput Biol. 15(4):1–28. doi:10.1371/journal.pcbi.1006650.

Brock JR, Dönmez AA, Beilstein MA, Olsen KM. 2018. Phylogenetics of Camelina Crantz. (Brassicaceae) and insights on the origin of gold-of-pleasure (Camelina sativa). Mol Phylogenet Evol. 127(April):834–842. doi:10.1016/j.ympev.2018.06.031. https://doi.org/10.1016/j.ympev.2018.06.031.

Brock JR, Mandáková T, Lysak MA, Al-Shehbaz IA. 2019. *Camelina neglecta* (Brassicaceae, Camelineae), a new diploid species from Europe. PhytoKeys. 115:51–57. doi:10.3897/phytokeys.115.31704.

Burns R, Mandáková T, Gunis J, Soto-Jiménez LM, Liu C, Lysak MA, Novikova PY, Nordborg M. 2021. Gradual evolution of allopolyploidy in Arabidopsis suecica. Nat Ecol Evol. 5(10):1367–1381. doi:10.1038/s41559-021-01525-w.

Cao Z, Liu X, Ogilvie H, Yan Z, Nakhleh L. 2019. Practical Aspects of Phylogenetic Network Analysis Using PhyloNet. doi:10.1101/746362.

Chalhoub B, Denoeud F, Liu S, Parkin IAP, Tang H, Wang X, Chiquet J, Belcram H, Tong C, Samans B, et al. 2014. Early allopolyploid evolution in the post-Neolithic *Brassica napus* oilseed genome. Science (80-). 345(6199):950–953. doi:10.1126/science.1253435. http://www.sciencemag.org/cgi/doi/10.1126/science.1253435.

Chaudhary R, Koh CS, Kagale S, Tang L, Wu SW, Lv Z, Mason AS, Sharpe AG, Diederichsen A, Parkin IAP. 2020. Assessing diversity in the camelina genus provides insights into the genome structure of *Camelina sativa*. G3 Genes, Genomes, Genet. 10(4):1297–1308. doi:10.1534/g3.119.400957.

Chen H. 2021. VennDiagram: Generate High-Resolution Venn and Euler Plots. https://cran.r-project.org/package=VennDiagram.

Chen MY, Liang D, Zhang P. 2017. Phylogenomic resolution of the phylogeny of laurasiatherian mammals: Exploring phylogenetic signals within coding and noncoding sequences. Genome Biol Evol. 9(8):1998–2012. doi:10.1093/gbe/evx147.

Coombe L, Nikolić V, Chu J, Birol I, Warren RL. 2020. ntJoin: Fast and lightweight assembly-guided scaffolding using minimizer graphs. Bioinformatics. 36(12):3885–3887. doi:10.1093/bioinformatics/btaa253.

Crowl AA, Manos PS, McVay JD, Lemmon AR, Lemmon EM, Hipp AL. 2020. Uncovering the genomic signature of ancient introgression between white oak lineages (*Quercus*). New Phytol. 226(4):1158–1170. doi:10.1111/nph.15842.

Ellinghaus D, Kurtz S, Willhoeft U. 2008. LTRharvest, an efficient and flexible software for de novo detection of LTR retrotransposons. BMC Bioinformatics. 9. doi:10.1186/1471-2105-9-18.

Emms DM, Kelly S. 2017. STRIDE: Species tree root inference from gene duplication events. Mol Biol Evol. 34(12):3267–3278. doi:10.1093/molbev/msx259.

Emms DM, Kelly S. 2019. OrthoFinder: Phylogenetic orthology inference for comparative genomics. Genome Biol. 20(1):1–14. doi:10.1186/s13059-019-1832-y.

Ford-Lloyd B V, Schmidt M, Armstrong SJ, Barazani O, Engels J, Hadas R, Hammer K, Kell SP, Kang D, Khoshbakht K, et al. 2011. Crop wild relatives - Undervalued, underutilized and under threat? Bioscience. 61(7):559–565. doi:10.1525/bio.2011.61.7.10.

Greiner S, Lehwark P, Bock R. 2019. OrganellarGenomeDRAW (OGDRAW) version 1.3.1:

Expanded toolkit for the graphical visualization of organellar genomes. Nucleic Acids Res. 47(W1):W59–W64. doi:10.1093/nar/gkz238.

Gu Z, Gu L, Eils R, Schlesner M, Brors B. 2014. Circlize implements and enhances circular visualization in R. Bioinformatics. 30(19):2811–2812. doi:10.1093/bioinformatics/btu393.

Guiglielmoni N, Houtain A, Derzelle A, Van Doninck K, Flot JF. 2021. Overcoming uncollapsed haplotypes in long-read assemblies of non-model organisms. BMC Bioinformatics. 22(1):1–23. doi:10.1186/s12859-021-04118-3. https://doi.org/10.1186/s12859-021-04118-3.

Hao Z, Dekang L, Ge Y, Shi J, Dolf W, Yu G, Chen J. 2020. RIdeogram: Drawing SVG Graphics to Visualize and Map Genome-Wide Data on Idiograms. https://cran.r-project.org/package=RIdeogram.

Heibl C. 2008. PHYLOCH: R language tree plotting tools and interfaces to diverse phylogenetic software packages. http://www.christophheibl.de/Rpackages.html.

Hu K, Xu K, Wen J, Yi B, Shen J, Ma C, Fu T, Ouyang Y, Tu J. 2019. Helitron distribution in Brassicaceae and whole Genome Helitron density as a character for distinguishing plant species. BMC Bioinformatics. 20(1):1–20. doi:10.1186/s12859-019-2945-8.

Husband BC, Baldwin SJ, Suda J. 2013. The incidence of polyploid in natural plant populations: major patterns and evolutionary processses. In: Leitch IJ, Al. E, editors. Plant Genome Diversity. Springer-Verlag. p. 255–276. http://link.springer.com/10.1007/978-3-7091-1160-4.

Jiao Y, Peluso P, Shi J, Liang T, Stitzer MC, Wang B, Campbell MS, Stein JC, Wei X, Chin CS, et al. 2017. Improved maize reference genome with single-molecule technologies. Nature. 546(7659):524–527. doi:10.1038/nature22971. http://dx.doi.org/10.1038/nature22971.

Jones G. 2013. Bayesian phylogenetic analysis for diploid and allotetraploid species networks.

Kagale S, Koh C, Nixon J, Bollina V, Clarke WE, Tuteja R, Spillane C, Robinson SJ, Links MG, Clarke C, et al. 2014. The emerging biofuel crop *Camelina sativa* retains a highly undifferentiated hexaploid genome structure. Nat Commun. 5:3706–3717. doi:10.1038/ncomms4706. [accessed 2014 Aug 13]. http://www.pubmedcentral.nih.gov/articlerender.fcgi?artid=4015329&tool=pmcentrez&rendertype=abstract.

Kapitonov V V., Jurka J. 2001. Rolling-circle transposons in eukaryotes. Proc Natl Acad Sci U S A. 98(15):8714–8719. doi:10.1073/pnas.151269298.

Koch MA, Kiefer M. 2005. Genome evolution among cruciferous plants: a lecture from the comparison of the genetic maps to three diploid species - Capsella rubella, Arabidopsis lyrata subsp. petraea, and A. thaliana. Am J Bot. 92(4):761–767.

Komsta L. 2011. outliers: Tests for outliers.

Koren S, Walenz BP, Berlin K, Miller JR, Phillippy AM. 2016. Canu: scalable and accurate long-read assembly via adaptive k-mer weighting and repeat separation. bioRxiv. doi:10.1101/071282.

Kyriakidou M, Tai HH, Anglin NL, Ellis D, Strömvik M V. 2018. Current Strategies of Polyploid Plant Genome Sequence Assembly. Front Plant Sci. 9(November):1660–1675. doi:10.3389/fpls.2018.01660. https://www.frontiersin.org/article/10.3389/fpls.2018.01660/full.

Langmead B, Salzberg SL. 2012. Fast gapped-read alignment with Bowtie 2. Nat Methods.

9(4):357–359. doi:10.1038/nmeth.1923.Fast.

Latta RG, Bekele WA, Wight CP, Tinker NA. 2019. Comparative linkage mapping of diploid, tetraploid, and hexaploid *Avena* species suggests extensive chromosome rearrangement in ancestral diploids. Sci Rep. 9(1):1–12. doi:10.1038/s41598-019-48639-7. http://dx.doi.org/10.1038/s41598-019-48639-7.

Lawrence M, Huber W, Pagès H, Aboyoun P, Carlson M, Gentleman R, Morgan M, Carey V. 2013. Software for computing and annotating genomic ranges. PLoS Comput Biol. 9. doi:10.1371/journal.pcbi.1003118.

Lemon J. 2006. Plotrix: a package in the red light district of R. R-News. 6(4):8–12.

Levin DA. 1983. Polyploidy and novelty in flowering plants. Am Nat. 122(1):1–25.

Li H. 2013. Aligning sequence reads, clone sequences and assembly contigs with BWA-MEM. 00(00):1–3. http://arxiv.org/abs/1303.3997.

Li H, Handsaker B, Wysoker A, Fennell T, Ruan J, Homer N, Marth G, Abecasis G, Durbin R. 2009. The Sequence Alignment/Map format and SAMtools. Bioinformatics. 25(16):2078–2079. doi:10.1093/bioinformatics/btp352.

Lujan Toro BE. 2017. Genome assembly of Camelina microcarpa Andrz. Ex DC, A step towards understanding genome evolution in Camelina. Carleton University.

Lysak MA, Mandakova T, Schranz ME. 2016. Comparative paleogenomics of crucifers: Ancestral genomic blocks revisited. Curr Opin Plant Biol. 30:108–115. doi:10.1016/j.pbi.2016.02.001.

Madlung A, Tyagi AP, Watson B, Jiang H, Kagochi T, Doerge RW, Martienssen R, Comai L. 2005. Genomic changes in synthetic *Arabidopsis* polyploids. Plant J. 41(2):221–230. doi:10.1111/j.1365-313X.2004.02297.x.

Mahmoud M, Doddapaneni H, Timp W, Sedlazeck FJ. 2021. PRINCESS: comprehensive detection of haplotype resolved SNVs, SVs, and methylation. Genome Biol. 22(1):1–17. doi:10.1186/s13059-021-02486-w.

Manca A, Pecchia P, Mapelli S, Masella P, Galasso I. 2013. Evaluation of genetic diversity in a *Camelina sativa* (L.) Crantz collection using microsatellite markers and biochemical traits. Genet Resour Crop Evol. 60(4):1223–1236. doi:10.1007/s10722-012-9913-8.

Mandáková T, Pouch M, Brock JR, Al-Shehbaz IA, Lysak MA. 2019. Origin and Evolution of Diploid and Allopolyploid Camelina Genomes Were Accompanied by Chromosome Shattering. Plant Cell. 31(11):2596–2612. doi:10.1105/tpc.19.00366.

Marcussen T, Sandve SR, Heier L, Pfeifer M, Kugler KG, Zhan B, Spannagl M, Pfeifer M, Jakobsen KS, Wulff BBH, et al. 2014. Ancient hybridizations among the ancestral genomes of bread wheat. Science. 345(6194):1250092. doi:10.1126/science.1251788. http://www.sciencemag.org/content/345/6194/1250092.abstract.

Martin SH, Davey JW, Jiggins CD. 2015. Evaluating the use of ABBA-BABA statistics to locate introgressed loci. Mol Biol Evol. 32(1):244–257. doi:10.1093/molbev/msu269.

Martin SH, Jiggins CD. 2017. Interpreting the genomic landscape of introgression. Curr Opin Genet Dev. 47:69–74. doi:10.1016/j.gde.2017.08.007.

Martin SL. 2017. An update to the Canadian range, abundance, and ploidy of Camelina spp.

(Brassicaceae) east of the Rocky Mountains. Botany.:1–13. doi:10.1139/cjb-2016-0070.

Martin SL, Smith T, James T, Shalabi F, Kron P, Sauder CA. 2017. An update to the Canadian range and abundance of Camelina spp. (Brassicaceae) east of the Rocky Mountains. Botany. 95:405–417.

Michael TP, VanBuren R. 2015. Progress, challenges and the future of crop genomes. Curr Opin Plant Biol. 24:71–81. doi:10.1016/j.pbi.2015.02.002. http://dx.doi.org/10.1016/j.pbi.2015.02.002.

Morgan M, Pagès H, Obenchain V, Hayden N. 2020. Rsamtools: Binary alignment (BAM), FASTA, variant call (BCF), and tabix file import. http://bioconductor.org/packages/Rsamtools.

Murat F, Louis A, Maumus F, Armero A, Cooke R, Quesneville H, Crollius HR, Salse J. 2015. Understanding Brassicaceae evolution through ancestral genome reconstruction. Genome Biol. 16(1):262. doi:10.1186/s13059-015-0814-y. http://genomebiology.com/2015/16/1/262.

Nikolov LA, Shushkov P, Nevado B, Gan X, Al-Shehbaz IA, Filatov D, Bailey CD, Tsiantis M. 2019. Resolving the backbone of the Brassicaceae phylogeny for investigating trait diversity. New Phytol. 222(3):1638–1651. doi:10.1111/nph.15732.

Oddes S, Zelig A, Kaplan N. 2018. Three invariant Hi-C interaction patterns: Applications to genome assembly. bioRxiv. 142:89–99. doi:10.1016/j.ymeth.2018.04.013.

Ogilvie HA, Bouckaert RR, Drummond AJ. 2017. StarBEAST2 brings faster species tree inference and accurate estimates of substitution rates. Mol Biol Evol. 34(8):2101–2114. doi:10.1093/molbev/msx126.

Otto SP, Whitton J. 2002. Polyploid Incidence and Evolution. Annu Rev Genet. 34(1):401–437. doi:10.1146/annurev.genet.34.1.401.

Ou S, Chen J, Jiang N. 2018. Assessing genome assembly quality using the LTR Assembly Index (LAI). Nucleic Acids Res. 46(21):e126. doi:10.1093/nar/gky730.

Ou S, Jiang N. 2018. LTR_retriever: A highly accurate and sensitive program for identification of long terminal repeat retrotransposons. Plant Physiol. 176(2):1410–1422. doi:10.1104/pp.17.01310.

Ou S, Jiang N. 2019. LTR_FINDER_parallel: Parallelization of LTR_FINDER enabling rapid identification of long terminal repeat retrotransposons. Mob DNA. 10(1):1–3. doi:10.1186/s13100-019-0193-0.

Ou S, Su W, Liao Y, Chougule K, Agda JRA, Hellinga AJ, Lugo CSB, Elliott TA, Ware D, Peterson T, et al. 2019. Benchmarking transposable element annotation methods for creation of a streamlined, comprehensive pipeline. Genome Biol. 20(1):1–18. doi:10.1186/s13059-019-1905-y.

Pagès H, Aboyoun P, Gentleman R, DebRoy S. 2020. Biostrings: Efficient manipulation of biological. https://bioconductor.org/packages/release/bioc/html/Biostrings.html.

Paradis E, Schliep K. 2019. ape 5.0: an environment for modern phylogenetics and evolutionary analyses in R. Bioinformatics. 35:526–528.

Parisod C, Senerchia N. 2012. Responses of Transposable Elements to Polyploidy. In: Topics in Current Genetics. Vol. 24. Springer-Verlag Berlin Heidelberg. p. 147–168. http://link.springer.com/10.1007/978-1-62703-568-2.

Pires CJ, Zhao J, Schranz ME, Leon EJ, Quijada PA, Lukens LN, Osborn TC. 2004. Flowering time divergence and genomic rearrangements in resynthesized *Brassica* polyploids (Brassicaceae). Biol J Linn Soc. 82(4):675–688. [accessed 2011 Apr 29]. http://www3.botany.ubc.ca/rieseberglab/plantevol/Piresetal2004.pdf.

Quesneville H. 2020. Twenty years of transposable element analysis in the Arabidopsis thaliana genome. Mob DNA. 11(1):1–13. doi:10.1186/s13100-020-00223-x.

Rambaut A. 2018. FigTree. tree.bio.ed.ac.uk/software/figtree/.

Rambaut A, Drummond AJ, Xie D, Baele G, Suchard MA. 2018. Posterior summarization in Bayesian phylogenetics using Tracer 1.7. Syst Biol. 67(5):901–904. doi:10.1093/sysbio/syy032.

Ramos-Madrigal J, Smith BD, Moreno-Mayar JV, Gopalakrishnan S, Ross-Ibarra J, Gilbert MTP, Wales N. 2016. Genome Sequence of a 5,310-Year-Old Maize Cob Provides Insights into the Early Stages of Maize Domestication. Curr Biol. 26(23):3195–3201. doi:10.1016/j.cub.2016.09.036.

Revell LJ. 2012. phytools: Phylogenetic tools for comparative biology (and other things). Methods Ecol Evol. 3:217–223. doi:10.1111/j.2041- 210X.2011.00169.x. https://cran.r-project.org/web/packages/phytools/index.html.

Rieseberg LH. 1997. Hybrid origins of plant species. Annu Rev Ecol Syst. 28(1):359–389. doi:10.1146/annurev.ecolsys.28.1.359. http://www.annualreviews.org/doi/10.1146/annurev.ecolsys.28.1.359.

Rieseberg LH. 2001. Chromosomal rearrangements and speciation. Trends Ecol Evol. 16(7):351–358. http://www.ncbi.nlm.nih.gov/pubmed/11403867.

Rieseberg LH, Willis JH. 2007. Plant speciation. Science. 317(5840):910–4. doi:10.1126/science.1137729. http://science.sciencemag.org/content/317/5840/910.abstract.

Roach MJ, Schmidt SA, Borneman AR. 2018. Purge Haplotigs: Allelic contig reassignment for third-gen diploid genome assemblies. BMC Bioinformatics. 19(1):1–10. doi:10.1186/s12859-018-2485-7.

Ronquist F, Teslenko M, Van Der Mark P, Ayres DL, Darling A, Höhna S, Larget B, Liu L, Suchard MA, Huelsenbeck JP. 2012. Mrbayes 3.2: Efficient bayesian phylogenetic inference and model choice across a large model space. Syst Biol. 61(3):539–542. doi:10.1093/sysbio/sys029.

Rothfels CJ. 2021. Polyploid phylogenetics. New Phytol. 230(1):66–72. doi:10.1111/nph.17105.

Sarilar V, Palacios PM, Rousselet A, Ridel C, Falque M, Eber F, Chèvre AM, Joets J, Brabant P, Alix K. 2013. Allopolyploidy has a moderate impact on restructuring at three contrasting transposable element insertion sites in resynthesized Brassica napus allotetraploids. New Phytol. 198(2):593–604. doi:10.1111/nph.12156.

Sato S, Tabata S, Hirakawa H, Asamizu E, Shirasawa K, Isobe S, Kaneko T, Nakamura Y, Shibata D, Aoki K, et al. 2012. The tomato genome sequence provides insights into fleshy fruit evolution. Nature. 485(7400):635–641. doi:10.1038/nature11119.

Schliep K, Jombart T, Kamvar ZN, Archer E, Harris R. 2020. apex: Phylogenetic Methods for Multiple Gene Data. https://cran.r-project.org/package=apex%7D.

Schliep KP. 2011. phangorn□: phylogenetic analysis in R. Bioinformatics. 27(4):592–593. doi:10.1093/bioinformatics/btq706.

Schmutz J, Cannon SB, Schlueter J, Ma J, Mitros T, Nelson W, Hyten DL, Song Q, Thelen JJ, Cheng J, et al. 2010. Genome sequence of the palaeopolyploid soybean. Nature. 463(7278):178–183. doi:10.1038/nature08670.

Schnable JC, Springer NM, Freeling M. 2011. Differentiation of the maize subgenomes by genome dominance and both ancient and ongoing gene loss. Proc Natl Acad Sci. 108(10):4069–4074. doi:10.1073/pnas.1101368108. http://www.pnas.org/cgi/doi/10.1073/pnas.1101368108.

Schnable PS, Pasternak S, Liang C, Zhang J, Fulton L, Graves TA, Minx P, Reily AD, Courtney L, Kruchowski SS, et al. 2009. The B73 Maize Genome: Complexity, Diversity, and Dynamics. Science (80-). 326(June):1112–1115.

Schranz ME, Lysak M a., Mitchell-Olds T. 2006. The ABC's of comparative genomics in the Brassicaceae: building blocks of crucifer genomes. Trends Plant Sci. 11(11):535–542. doi:10.1016/j.tplants.2006.09.002.

Schulz A. 2021. pBrackets: Plot Brackets. https://cran.r-project.org/package=pBrackets.

Simão FA, Waterhouse RM, Ioannidis P, Kriventseva E V, Zdobnov EM. 2015. BUSCO: Assessing genome assembly and annotation completeness with single-copy orthologs. Bioinformatics. 31(19):3210–3212. doi:10.1093/bioinformatics/btv351.

Soltis D, Soltis P. 1999. Polyploidy: recurrent formation and genome evolution. Trends Ecol Evol. 14(9):348–352. http://www.ncbi.nlm.nih.gov/pubmed/10441308.

Soltis PS, Soltis DE. 2009. The role of hybridization in plant speciation. Annu Rev Plant Biol. 60:561–88. doi:10.1146/annurev.arplant.043008.092039. http://www.ncbi.nlm.nih.gov/pubmed/19575590.

Stanke M, Schöffmann O, Morgenstern B, Waack S. 2006. Gene prediction in eukaryotes with a generalized hidden Markov model that uses hints from external sources. BMC Bioinformatics. 7:1–11. doi:10.1186/1471-2105-7-62.

Stebbins GL. 1968. The significance of hybridization for plant taxonomy and evolution. Taxon. 18(1):26–35.

Struck TH. 2014. Trespex-detection of misleading signal in phylogenetic reconstructions based on tree information. Evol Bioinforma. 10:51–67. doi:10.4137/EBo.s14239.

Suchard MA, Lemey P, Baele G, Ayres DL, Drummond AJ, Rambaut A. 2018. Bayesian phylogenetic and phylodynamic data integration using BEAST 1.10. Virus Evol. 4(1):1–5. doi:10.1093/ve/vey016.

Than C, Ruths D, Nakhleh L. 2008. PhyloNet: A software package for analyzing and reconstructing reticulate evolutionary relationships. BMC Bioinformatics. 9:1–16. doi:10.1186/1471-2105-9-322.

The International Wheat Genome Sequencing Consortium. 2014. A chromosome-based draft sequence of the hexaploid bread wheat (*Triticum aestivum*) genome. Science. 345(6194):1251788. doi:10.1126/science.1251788. http://www.sciencemag.org/content/345/6194/1250092.abstract.

Tillich M, Lehwark P, Pellizzer T, Ulbricht-Jones ES, Fischer A, Bock R, Greiner S. 2017. GeSeq - Versatile and accurate annotation of organelle genomes. Nucleic Acids Res. 45(W1):W6–W11. doi:10.1093/nar/gkx391.

Vicient CM, Casacuberta JM. 2017. Impact of transposable elements on polyploid plant genomes. Ann Bot. 120(2):195–207. doi:10.1093/aob/mcx078.

Walker BJ, Abeel T, Shea T, Priest M, Abouelliel A, Sakthikumar S, Cuomo CA, Zeng Q, Wortman J, Young SK, et al. 2014. Pilon: An integrated tool for comprehensive microbial variant detection and genome assembly improvement. PLoS One. 9(11):e112963. doi:10.1371/journal.pone.0112963.

Wang L-G, Lam TT-Y, Xu S, Dai Z, Zhou L, Feng T, Guo P, Dunn CW, Jones BR, Bradley T, et al. 2020. treeio: an R package for phylogenetic tree input and output with richly annotated and associated data. Mol Biol Evol. 37(2):599–603. doi:10.1093/molbev/msz240.

Warren DL, Geneva AJ, Lanfear R, Rosenberg M. 2017. RWTY (R We There Yet): An R package for examining convergence of Bayesian phylogenetic analyses. Mol Biol Evol. 34(4):1016–1020. doi:10.1093/molbev/msw279.

Wen D, Yu Y, Zhu J, Nakhleh L. 2018. Inferring phylogenetic networks using PhyloNet. Syst Biol. 67(4):735–740. doi:10.1093/sysbio/syy015.

de Wet JMJ. 1971. Polyploidy and evolution in plants. Taxon. 20(1):29–35.

Wick RR, Judd LM, Holt KE. 2019. Performance of neural network basecalling tools for Oxford Nanopore sequencing. Genome Biol. 20(1):1–10. doi:10.1186/s13059-019-1727-y.

Wickham H. 2011. The split-apply-combine strategy for data analysis. J Stat Softw. 20(1):1–29. http://www.jstatsoft.org/v40/i01/.

Wickham H. 2019. stringr: simple, consistent wrappers for common string operations. https://cran.r-project.org/package=stringr.

Workman R, Fedak R, Kilburn D, Hao S, Liu K, Timp W. 2018. High molecular weight DNA extraction from recalcitrant plant species for third generation sequencing. Protoc Exch. version 1:1–15. doi:10.1038/protex.2018.059.

Wright K. 2021. pals: Color Palettes, Colormaps, and Tools to Evaluate Them.

Xu Z, Wang H. 2007. LTR-FINDER: An efficient tool for the prediction of full-length LTR retrotransposons. Nucleic Acids Res. 35(SUPPL.2):265–268. doi:10.1093/nar/gkm286.

Yu Q, Guyot R, De Kochko A, Byers A, Navajas-Pérez R, Langston BJ, Dubreuil-Tranchant C, Paterson AH, Poncet V, Nagai C, et al. 2011. Micro-collinearity and genome evolution in the vicinity of an ethylene receptor gene of cultivated diploid and allotetraploid coffee species (*Coffea*). Plant J. 67(2):305–317. doi:10.1111/j.1365-313X.2011.04590.x.

Žerdoner Čalasan A, Seregin AP, Hurka H, Hofford NP, Neuffer B. 2019. The Eurasian steppe belt in time and space: Phylogeny and historical biogeography of the false flax (*Camelina* Crantz, Camelineae, Brassicaceae). Flora Morphol Distrib Funct Ecol Plants. 260(October):151477. doi:10.1016/j.flora.2019.151477. https://doi.org/10.1016/j.flora.2019.151477.

Zhang C, Rabiee M, Sayyari E, Mirarab S. 2018. ASTRAL-III: Polynomial time species tree reconstruction from partially resolved gene trees. BMC Bioinformatics. 19(Suppl 6):15–30. doi:10.1186/s12859-018-2129-y. http://dx.doi.org/10.1186/s12859-018-2129-y.

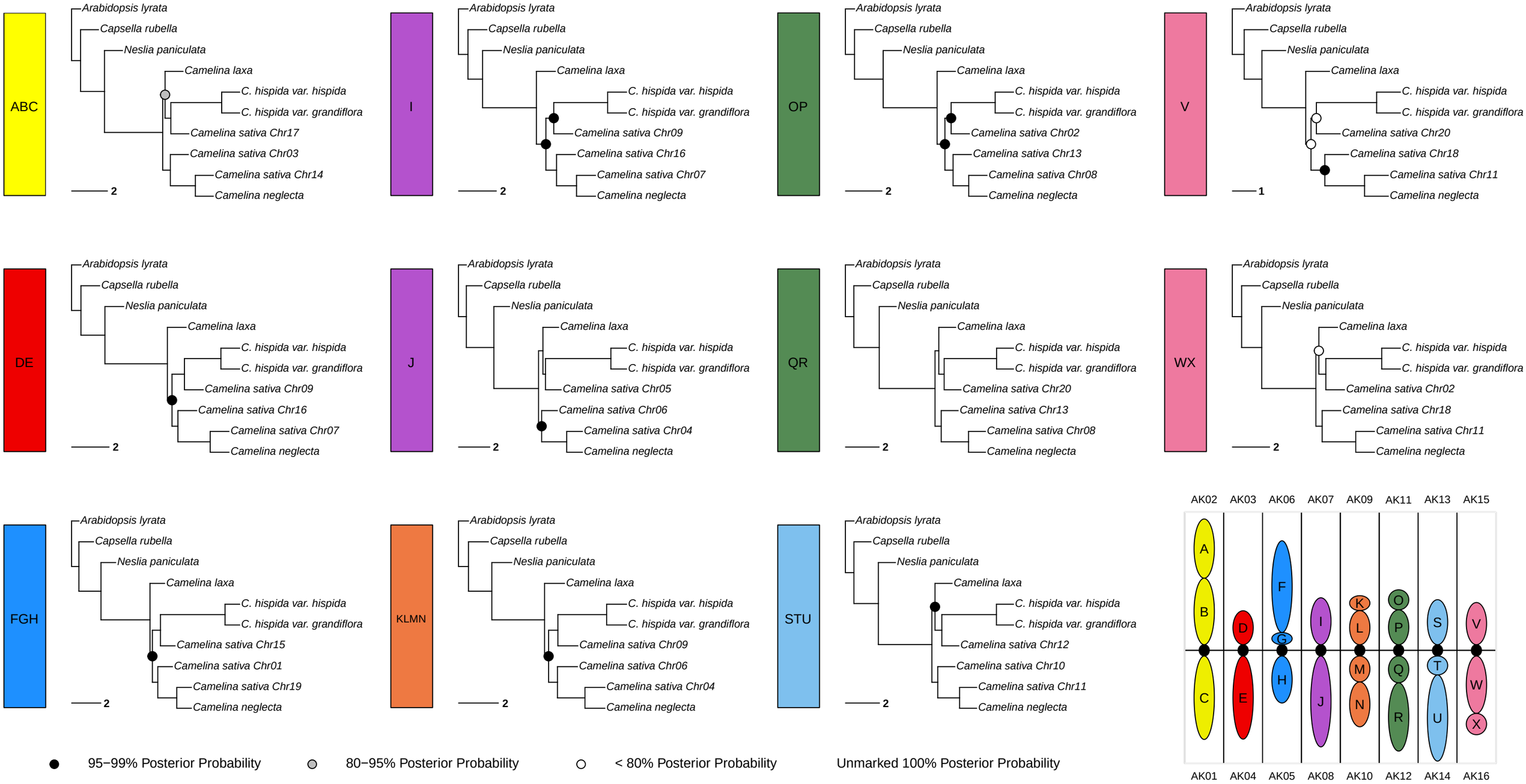
ABC
Arabidopsis lyrata
Capsella rubella
Neslia paniculata
Camelina laxa
C. hispida var. hispida
C. hispida var. grandiflora
Camelina sativa Chr17
Camelina sativa Chr03
Camelina sativa Chr14
Camelina neglecta
2
I
Arabidopsis lyrata
Capsella rubella
Neslia paniculata
Camelina laxa
C. hispida var. hispida
C. hispida var. grandiflora
Camelina sativa Chr09
Camelina sativa Chr16
Camelina sativa Chr07
Camelina neglecta
2
OP
Arabidopsis lyrata
Capsella rubella
Neslia paniculata
Camelina laxa
C. hispida var. hispida
C. hispida var. grandiflora
Camelina sativa Chr02
Camelina sativa Chr13
Camelina sativa Chr08
Camelina neglecta
2
V
Arabidopsis lyrata
Capsella rubella
Neslia paniculata
Camelina laxa
C. hispida var. hispida
C. hispida var. grandiflora
Camelina sativa Chr20
Camelina sativa Chr18
Camelina sativa Chr11
Camelina neglecta
1
DE
Arabidopsis lyrata
Capsella rubella
Neslia paniculata
Camelina laxa
C. hispida var. hispida
C. hispida var. grandiflora
Camelina sativa Chr09
Camelina sativa Chr16
Camelina sativa Chr07
Camelina neglecta
2
J
Arabidopsis lyrata
Capsella rubella
Neslia paniculata
Camelina laxa
C. hispida var. hispida
C. hispida var. grandiflora
Camelina sativa Chr05
Camelina sativa Chr06
Camelina sativa Chr04
Camelina neglecta
2
QR
Arabidopsis lyrata
Capsella rubella
Neslia paniculata
Camelina laxa
C. hispida var. hispida
C. hispida var. grandiflora
Camelina sativa Chr20
Camelina sativa Chr13
Camelina sativa Chr08
Camelina neglecta
2
WX
Arabidopsis lyrata
Capsella rubella
Neslia paniculata
Camelina laxa
C. hispida var. hispida
C. hispida var. grandiflora
Camelina sativa Chr02
Camelina sativa Chr18
Camelina sativa Chr11
Camelina neglecta
2
FGH
Arabidopsis lyrata
Capsella rubella
Neslia paniculata
Camelina laxa
C. hispida var. hispida
C. hispida var. grandiflora
Camelina sativa Chr15
Camelina sativa Chr01
Camelina sativa Chr19
Camelina neglecta
2
KLMN
Arabidopsis lyrata
Capsella rubella
Neslia paniculata
Camelina laxa
C. hispida var. hispida
C. hispida var. grandiflora
Camelina sativa Chr09
Camelina sativa Chr06
Camelina sativa Chr04
Camelina neglecta
2
STU
Arabidopsis lyrata
Capsella rubella
Neslia paniculata
Camelina laxa
C. hispida var. hispida
C. hispida var. grandiflora
Camelina sativa Chr12
Camelina sativa Chr10
Camelina sativa Chr11
Camelina neglecta
2
95−99% Posterior Probability
80−95% Posterior Probability
< 80% Posterior Probability
Unmarked 100% Posterior Probability
AK02 AK03 AK06 AK07 AK09 AK11 AK13 AK15
A B C D E F G H I J K L M N O P Q R S T U V W X
AK01 AK04 AK05 AK08 AK10 AK12 AK14 AK16

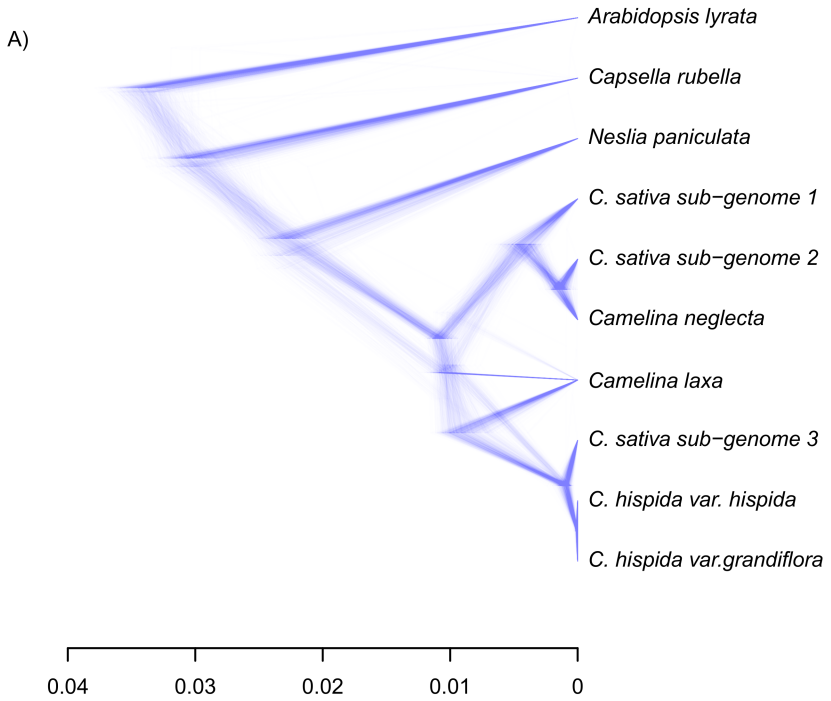
A)
Arabidopsis lyrata
Capsella rubella
Neslia paniculata
C. sativa sub−genome 1
C. sativa sub−genome 2
Camelina neglecta
Camelina laxa
C. sativa sub−genome 3
C. hispida var. hispida
C. hispida var.grandiflora
0.04
0.03
0.02
0.01
0

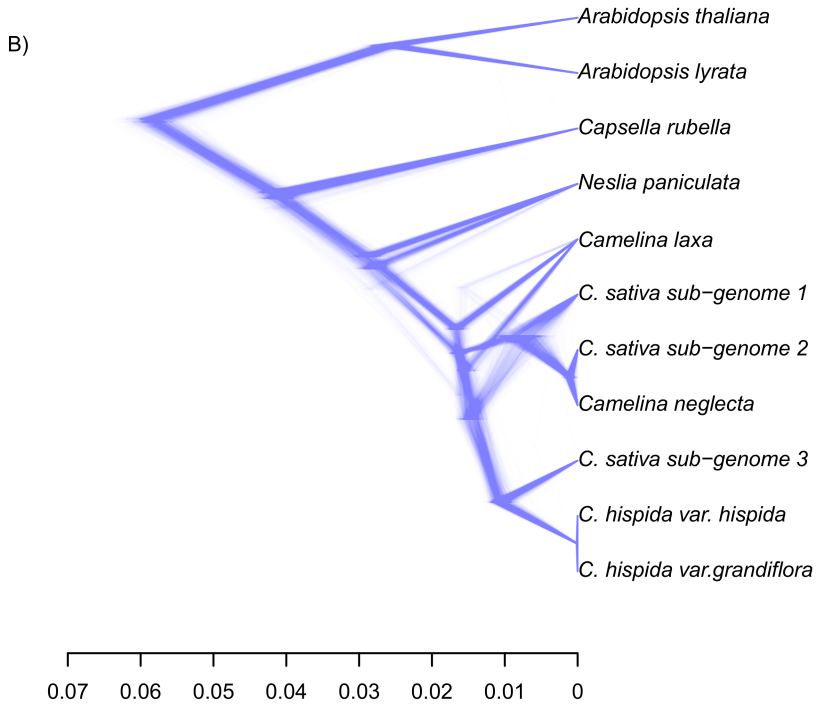
B)
Arabidopsis thaliana
Arabidopsis lyrata
Capsella rubella
Neslia paniculata
Camelina laxa
C. sativa sub−genome 1
C. sativa sub−genome 2
Camelina neglecta
C. sativa sub−genome 3
C. hispida var. hispida
C. hispida var.grandiflora
0.07
0.06
0.05
0.04
0.03
0.02
0.01
0

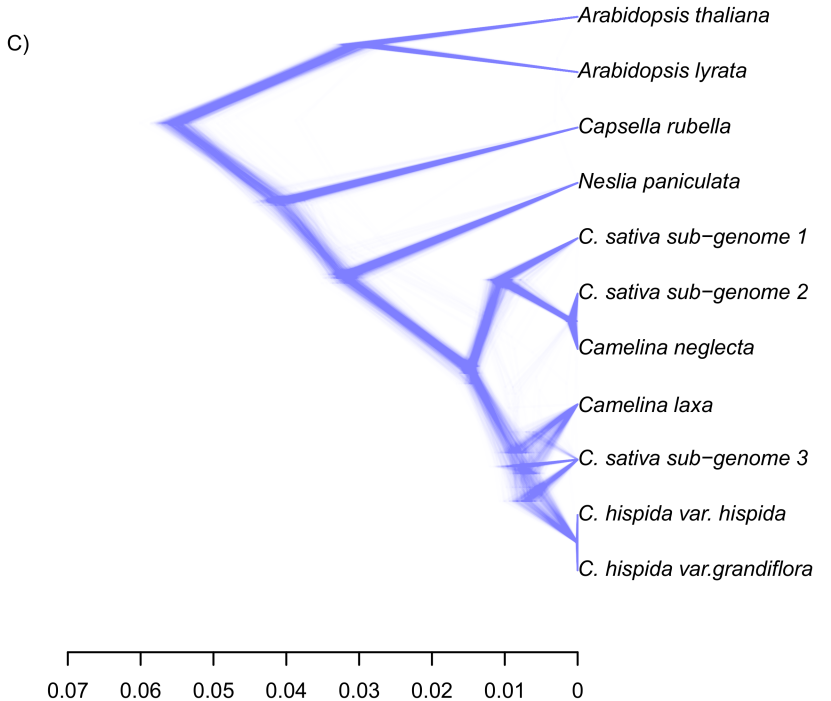
C)
Arabidopsis thaliana
Arabidopsis lyrata
Capsella rubella
Neslia paniculata
C. sativa sub−genome 1
C. sativa sub−genome 2
Camelina neglecta
Camelina laxa
C. sativa sub−genome 3
C. hispida var. hispida
C. hispida var.grandiflora
0.07
0.06
0.05
0.04
0.03
0.02
0.01
0

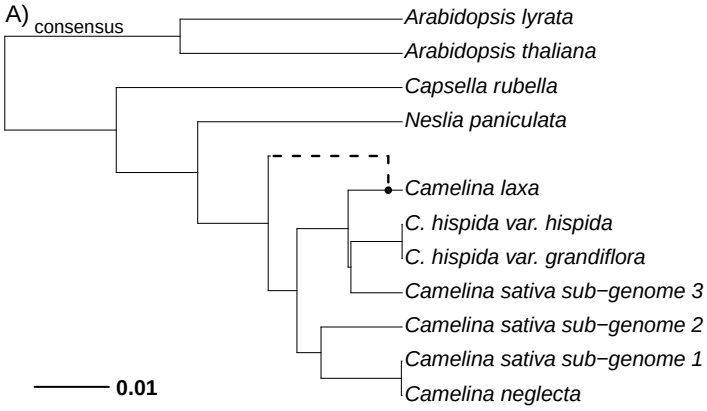
A)
consensus
Arabidopsis lyrata
Arabidopsis thaliana
Capsella rubella
Neslia paniculata
Camelina laxa
C. hispida var. hispida
C. hispida var. grandiflora
Camelina sativa sub−genome 3
Camelina sativa sub−genome 2
Camelina sativa sub−genome 1
Camelina neglecta
0.01

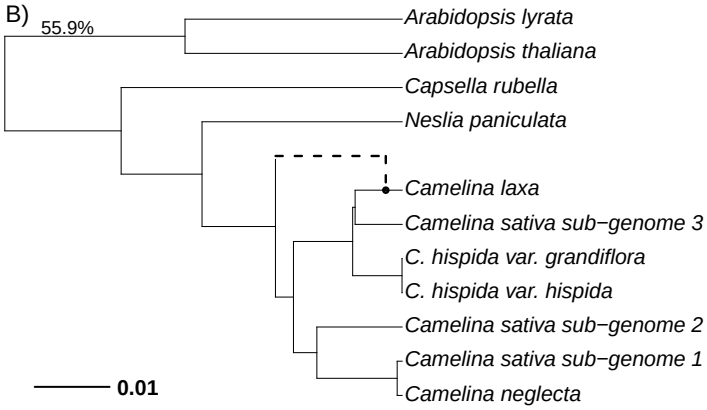
B)
55.9%
Arabidopsis lyrata
Arabidopsis thaliana
Capsella rubella
Neslia paniculata
Camelina laxa
Camelina sativa sub−genome 3
C. hispida var. grandiflora
C. hispida var. hispida
Camelina sativa sub−genome 2
Camelina sativa sub−genome 1
Camelina neglecta
0.01

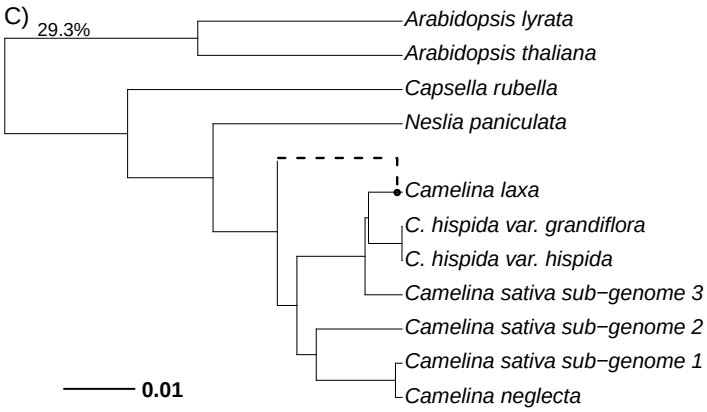
C)
29.3%
Arabidopsis lyrata
Arabidopsis thaliana
Capsella rubella
Neslia paniculata
Camelina laxa
C. hispida var. grandiflora
C. hispida var. hispida
Camelina sativa sub−genome 3
Camelina sativa sub−genome 2
Camelina sativa sub−genome 1
Camelina neglecta
0.01

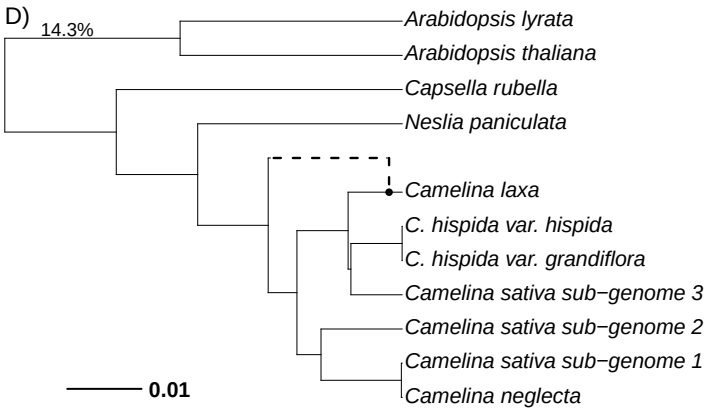
D)
14.3%
Arabidopsis lyrata
Arabidopsis thaliana
Capsella rubella
Neslia paniculata
Camelina laxa
C. hispida var. hispida
C. hispida var. grandiflora
Camelina sativa sub−genome 3
Camelina sativa sub−genome 2
Camelina sativa sub−genome 1
Camelina neglecta
0.01

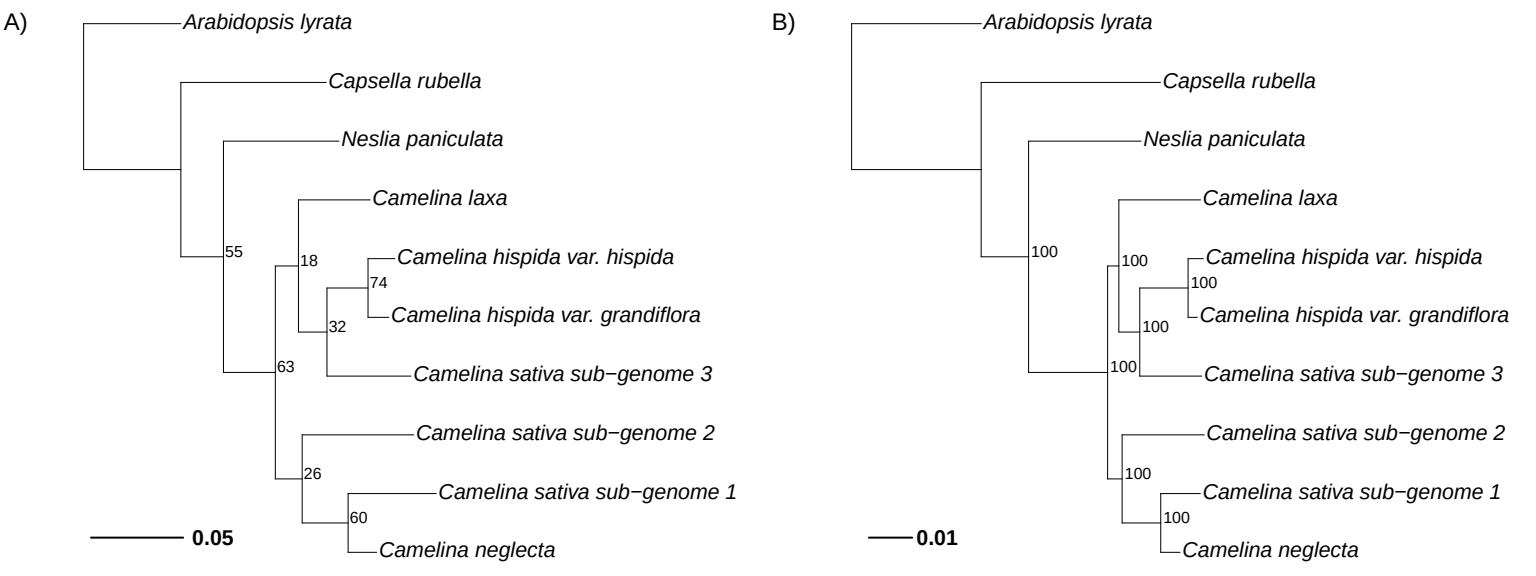
A)
Arabidopsis lyrata
Capsella rubella
Neslia paniculata
Camelina laxa
Camelina hispida var. hispida
Camelina hispida var. grandiflora
Camelina sativa sub−genome 3
Camelina sativa sub−genome 2
Camelina sativa sub−genome 1
Camelina neglecta
55
18
74
32
63
26
60
0.05
B)
Arabidopsis lyrata
Capsella rubella
Neslia paniculata
Camelina laxa
Camelina hispida var. hispida
Camelina hispida var. grandiflora
Camelina sativa sub−genome 3
Camelina sativa sub−genome 2
Camelina sativa sub−genome 1
Camelina neglecta
100
100
100
100
100
100
100
100
0.01

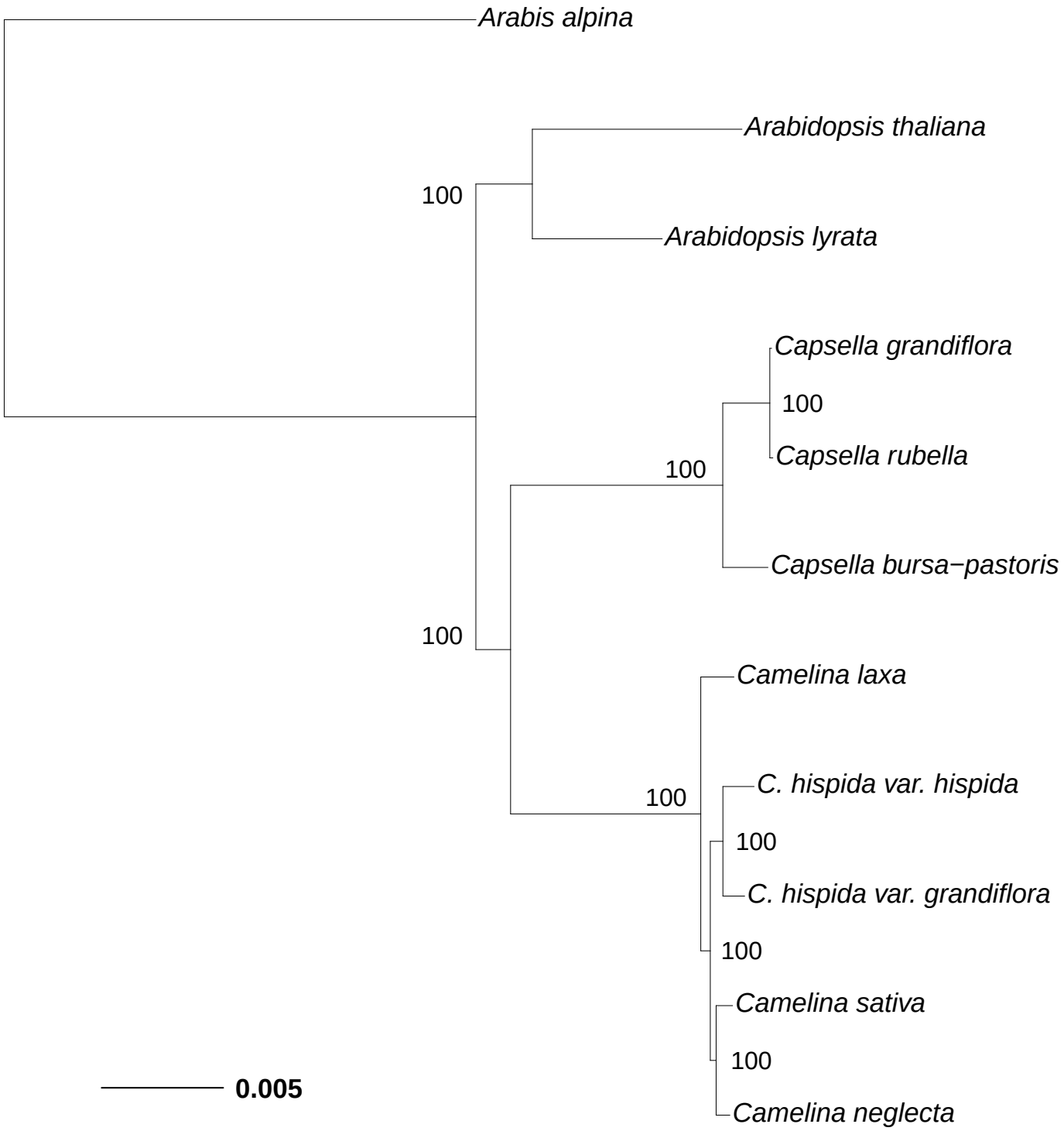
Arabis alpina
Arabidopsis thaliana
100
Arabidopsis lyrata
Capsella grandiflora
100
Capsella rubella
100
Capsella bursa−pastoris
100
Camelina laxa
C. hispida var. hispida
100
100
C. hispida var. grandiflora
100
Camelina sativa
100
Camelina neglecta
0.005

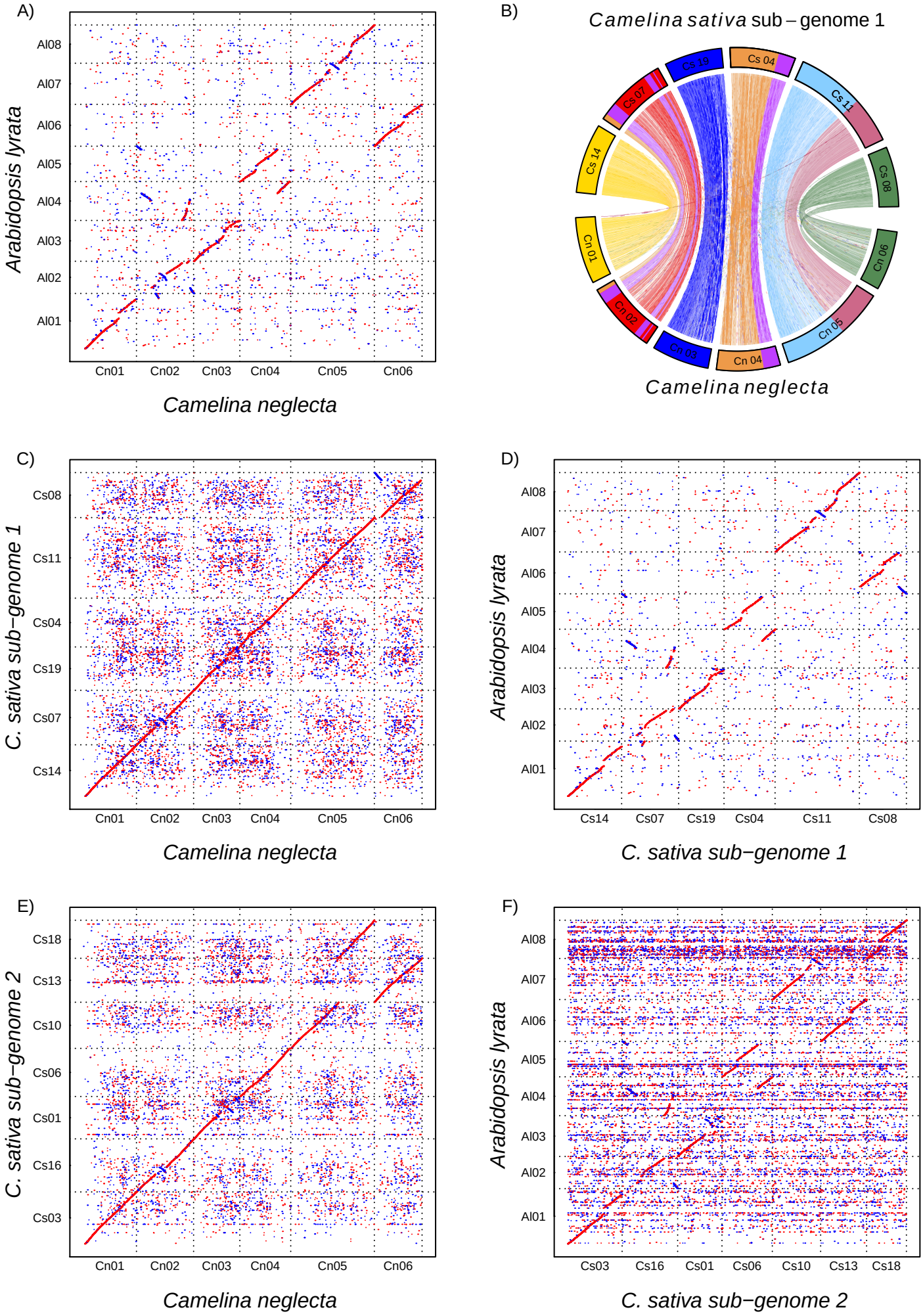
A)
Arabidopsis lyrata
Al08
Al07
Al06
Al05
Al04
Al03
Al02
Al01
Cn01
Cn02
Cn03
Cn04
Cn05
Cn06
Camelina neglecta
B)
Camelina sativa sub – genome 1
Cs 19
Cs 04
Cs 07
Cs 11
Cs 14
Cs 08
Cn 01
Cn 06
Cn 02
Cn 05
Cn 03
Cn 04
Camelina neglecta
C)
C. sativa sub−genome 1
Cs08
Cs11
Cs04
Cs19
Cs07
Cs14
Cn01
Cn02
Cn03
Cn04
Cn05
Cn06
Camelina neglecta
D)
Arabidopsis lyrata
Al08
Al07
Al06
Al05
Al04
Al03
Al02
Al01
Cs14
Cs07
Cs19
Cs04
Cs11
Cs08
C. sativa sub−genome 1
E)
C. sativa sub−genome 2
Cs18
Cs13
Cs10
Cs06
Cs01
Cs16
Cs03
Cn01
Cn02
Cn03
Cn04
Cn05
Cn06
Camelina neglecta
F)
Arabidopsis lyrata
Al08
Al07
Al06
Al05
Al04
Al03
Al02
Al01
Cs03
Cs16
Cs01
Cs06
Cs10
Cs13
Cs18
C. sativa sub−genome 2

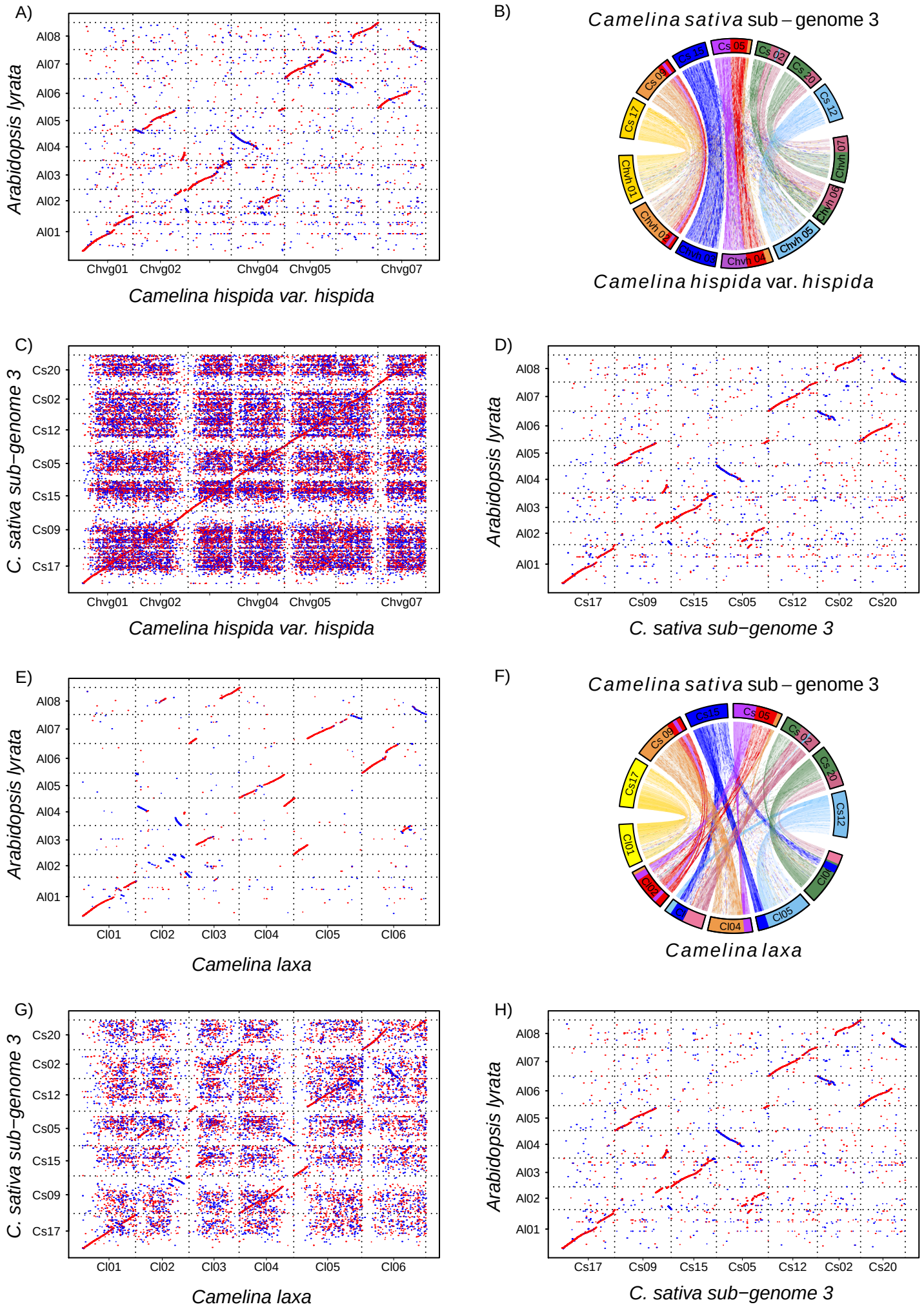
A)
Arabidopsis lyrata
Al08
Al07
Al06
Al05
Al04
Al03
Al02
Al01
Chvg01
Chvg02
Chvg04
Chvg05
Chvg07
Camelina hispida var. hispida
B)
Camelina sativa sub – genome 3
Cs 15
Cs 05
Cs 02
Cs 20
Cs 12
Cs 09
Cs 17
Chvh 07
Chvh 01
Chvh 06
Chvh 02
Chvh 05
Chvh 03
Chvh 04
Camelina hispida var. hispida
C)
C. sativa sub−genome 3
Cs20
Cs02
Cs12
Cs05
Cs15
Cs09
Cs17
Chvg01
Chvg02
Chvg04
Chvg05
Chvg07
Camelina hispida var. hispida
D)
Arabidopsis lyrata
Al08
Al07
Al06
Al05
Al04
Al03
Al02
Al01
Cs17
Cs09
Cs15
Cs05
Cs12
Cs02
Cs20
C. sativa sub−genome 3
E)
Arabidopsis lyrata
Al08
Al07
Al06
Al05
Al04
Al03
Al02
Al01
Cl01
Cl02
Cl03
Cl04
Cl05
Cl06
Camelina laxa
F)
Camelina sativa sub – genome 3
Cs 15
Cs 05
Cs 02
Cs 20
Cs 12
Cs 09
Cs17
Cl01
Cl02
Cl
Cl04
Cl05
Cl06
Camelina laxa
G)
C. sativa sub−genome 3
Cs20
Cs02
Cs12
Cs05
Cs15
Cs09
Cs17
Cl01
Cl02
Cl03
Cl04
Cl05
Cl06
Camelina laxa
H)
Arabidopsis lyrata
Al08
Al07
Al06
Al05
Al04
Al03
Al02
Al01
Cs17
Cs09
Cs15
Cs05
Cs12
Cs02
Cs20
C. sativa sub−genome 3

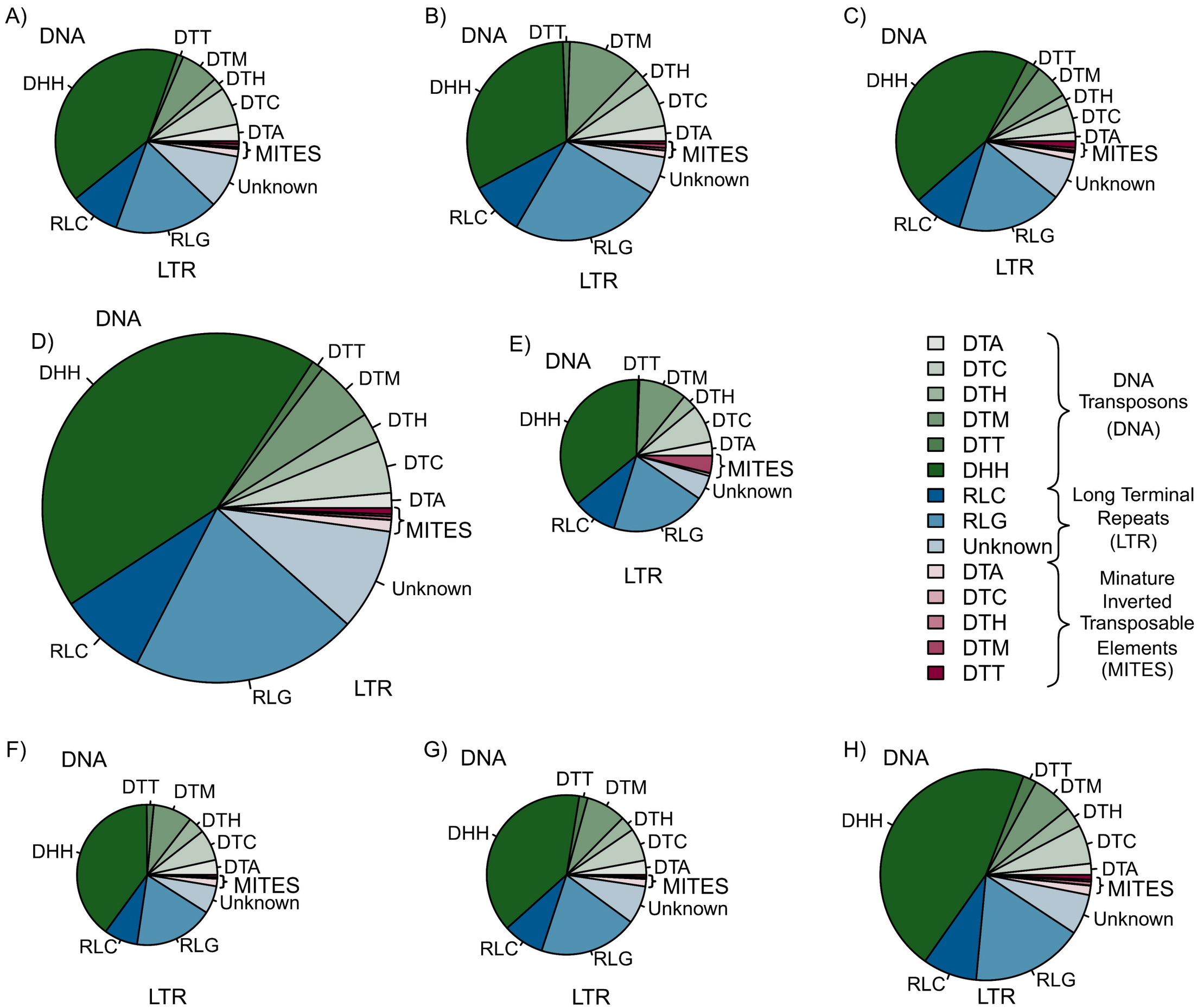
A)
DNA
DTT
DTM
DTH
DTC
DTA
MITES
Unknown
DHH
RLC
RLG
LTR
B)
DNA
DTT
DTM
DTH
DTC
DTA
MITES
Unknown
DHH
RLC
RLG
LTR
C)
DNA
DTT
DTM
DTH
DTC
DTA
MITES
Unknown
DHH
RLC
RLG
LTR
D)
DNA
DTT
DTM
DTH
DTC
DTA
MITES
Unknown
DHH
RLC
RLG
LTR
E)
DNA
DTT
DTM
DTH
DTC
DTA
MITES
Unknown
DHH
RLC
RLG
LTR
DTA
DTC
DTH
DTM
DTT
DHH
RLC
RLG
Unknown
DTA
DTC
DTH
DTM
DTT
DNA Transposons (DNA)
Long Terminal Repeats (LTR)
Minature Inverted Transposable Elements (MITES)
F)
DNA
DTT
DTM
DTH
DTC
DTA
MITES
Unknown
DHH
RLC
RLG
LTR
G)
DNA
DTT
DTM
DTH
DTC
DTA
MITES
Unknown
DHH
RLC
RLG
LTR
H)
DNA
DTT
DTM
DTH
DTC
DTA
MITES
Unknown
DHH
RLC
RLG
LTR

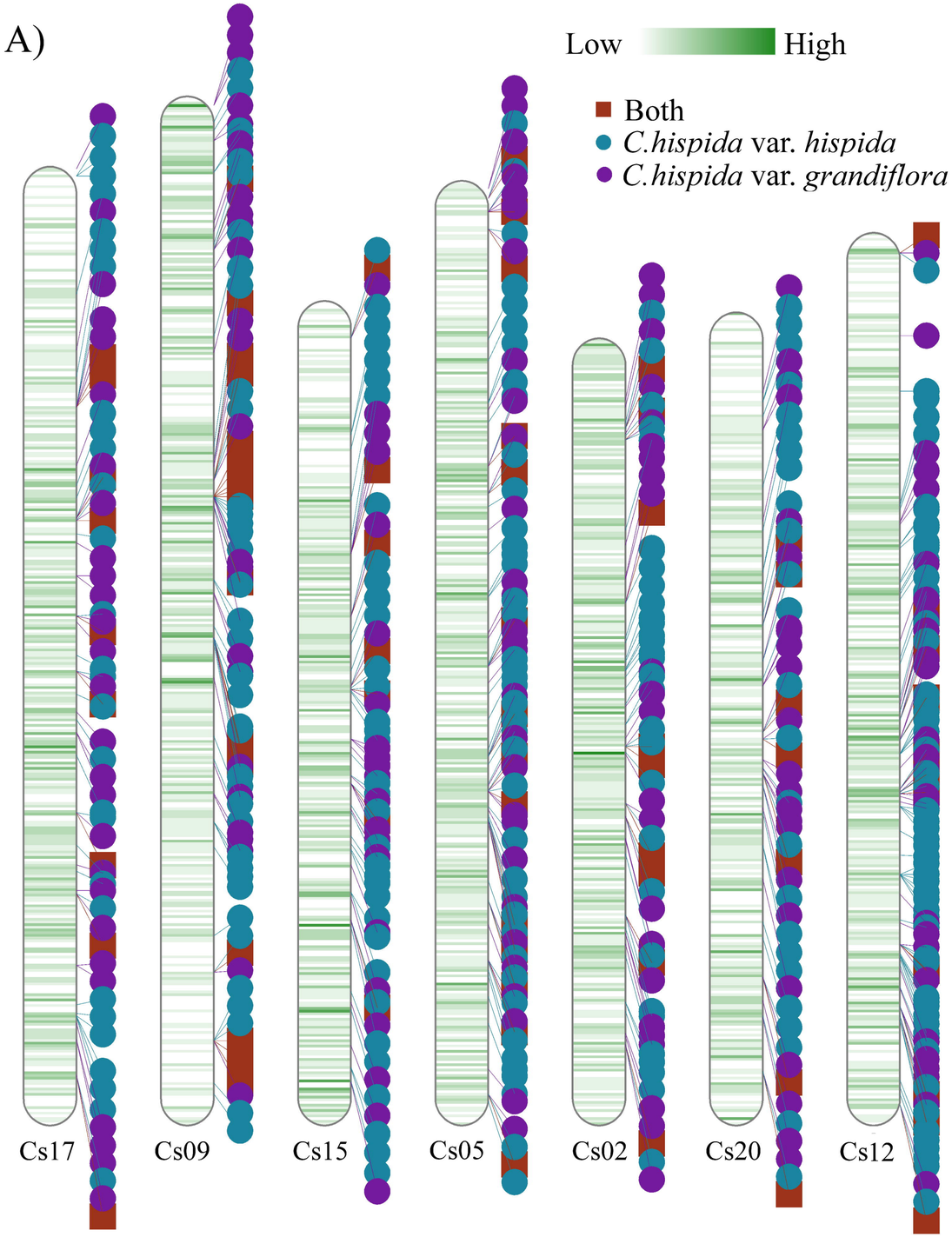
A)
Low
High
Both
C.hispida var. hispida
C.hispida var. grandiflora
Cs17
Cs09
Cs15
Cs05
Cs02
Cs20
Cs12

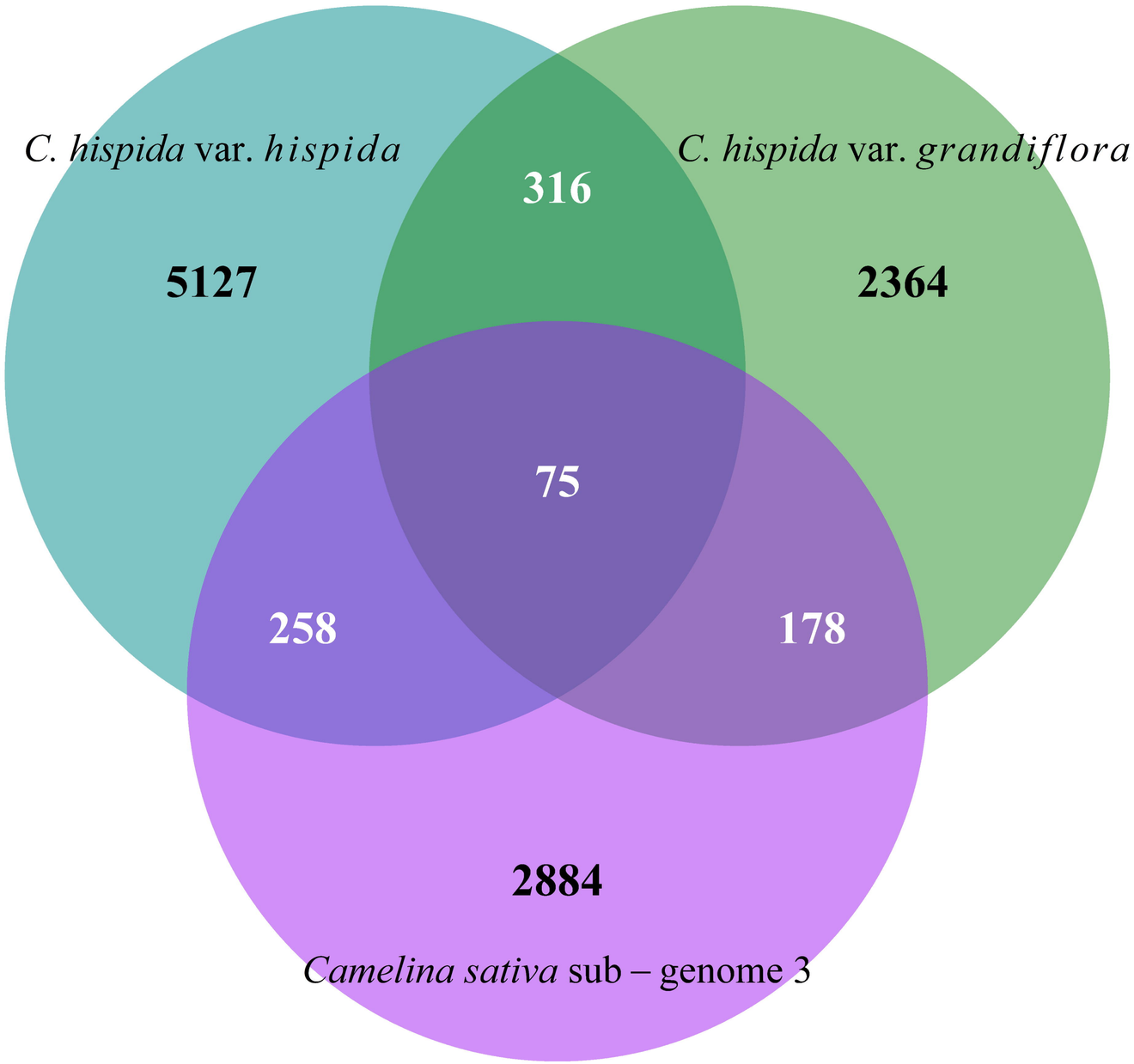
B)
C. hispida var. hispida
C. hispida var. grandiflora
Camelina sativa sub – genome 3
5127
316
2364
75
258
178
2884